energies

MDPI

Article

Thermodynamic Analysis and Optimization of Power Cycles for Waste Heat Recovery

Igor Maksimov [1], Vladimir Kindra [1,*], Andrey Vegera [1], Andrey Rogalev [1] and Nikolay Rogalev [2]

[1] Department of Innovative Technologies for High-Tech Industries, National Research University "Moscow Power Engineering Institute", 111250 Moscow, Russia; maksimovia98@gmail.com (I.M.); vegeraan@mpei.ru (A.V.); rogalevan@mpei.ru (A.R.)
[2] Department of Thermal Power Plants, National Research University "Moscow Power Engineering Institute", 111250 Moscow, Russia; rogalevnd@mpei.ru
* Correspondence: kindra.vladimir@yandex.ru

Abstract: Improvement of energy efficiency in technological processes at industrial enterprises is one of the key areas of energy saving. Reduction of energy costs required for the production of energy-intensive products can be achieved through the utilization of waste heat produced by high-temperature thermal furnace units. Generation of electric power based on the waste heat using power cycles with working fluids that are not conventional for large power engineering, may become a promising energy saving trend. In this paper, thermodynamic analysis and optimization of power cycles for the purposes of waste heat recovery are performed. The efficiency of combining several power cycles was also evaluated. It has been established that the combination of the Brayton recompression cycle on supercritical carbon dioxide with the organic Rankine cycle using R124 allows for greater electrical power than steam-power cycles with three pressure circuits under conditions where the gas temperature is in the range of 300–550 °C and the cooling temperature of is up to 80 °C. Additionally, when cooling gases with a high sulfur and moisture content to 150 °C, the combined cycle has greater electrical power at gas temperatures of 330 °C and above. At enterprises where the coolant has a high content of sulfur compounds or moisture and deep cooling of gases will lead to condensation, for example, at petrochemical and non-ferrous metallurgy enterprises, the use of combined cycles can ensure a utilization efficiency of up to 45%.

Keywords: waste heat; energy efficiency; organic Rankine cycle; Brayton cycle; heat recovery; thermodynamic optimization

check for updates

Citation: Maksimov, I.; Kindra, V.; Vegera, A.; Rogalev, A.; Rogalev, N. Thermodynamic Analysis and Optimization of Power Cycles for Waste Heat Recovery. *Energies* **2024**, *17*, 6375. https://doi.org/10.3390/en17246375

Academic Editor: George Kosmadakis

Received: 25 November 2024
Revised: 16 December 2024
Accepted: 17 December 2024
Published: 18 December 2024

Copyright: © 2024 by the authors. Licensee MDPI, Basel, Switzerland. This article is an open access article distributed under the terms and conditions of the Creative Commons Attribution (CC BY) license (https://creativecommons.org/licenses/by/4.0/).

1. Introduction

The global growth of power consumption caused by the active industrialization of developing countries, combined with the gradual depletion of fossil hydrocarbon fuel reserves, is a threat to sustainable development. Taking into account global climate change, improving environmental safety and energy efficiency in the main sectors of the world economy is one of the priority tasks.

Today, many countries around the world are adopting legislative acts aimed at tightening environmental standards and energy consumption requirements for various industries. Nowadays, the industrial sector remains one of the most energy-intensive sectors, and the issue of resource saving and increasing the use of energy efficiently is topical.

Following Eurostat data [1], in 2022, the total energy consumption by industry in the EU-27 countries amounted to more than 9450 PJ. Among the most energy-intensive industries, the chemical and petrochemical sector accounts for more than 20% of the total consumption, 14% comes from the non-metalliferous minerals mining and processing take, 13.5%—from the pulp and paper sector, 12%—from food production, and 10%—from iron and steel production (Figure 1).

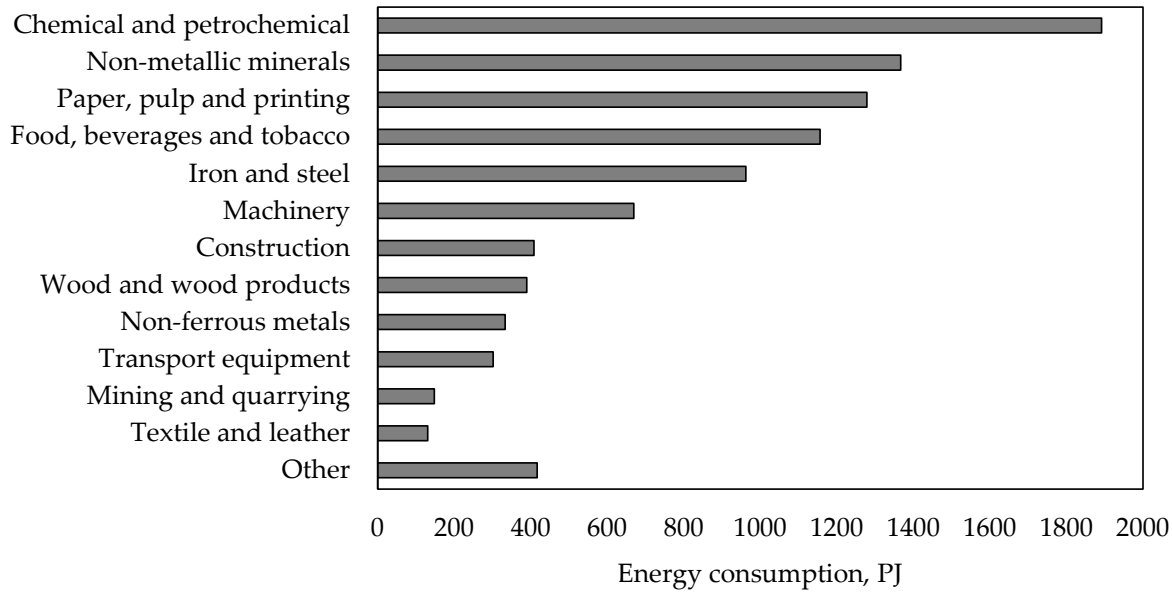


Figure 1. Final energy consumption by main industries in EU-27 countries in 2022.

The high level of energy consumption by industrial enterprises is caused by technological processes, among which the most energy-intensive are high-temperature processes. Vast amounts of heat consumed by high-temperature furnace plants, having temperatures much higher than ambient, contribute to sources of waste heat. This energy, generated in technological processes and often dissipated without any useful application, is a priority target among energy saving tasks. In the context of rising energy costs and tightening environmental requirements, the useful application of waste heat becomes quite vital.

The potential for energy savings from utilizing waste heat varies considerably, depending on the technological process. One of the criteria describing the potential for useful application of heat is the temperature of the source: the higher the temperature of the heat carrier in relation to the environment, the greater both the amount of energy that can be usefully applied and the efficiency of its possible use. Figure 2 presents information on the temperature of technological processes where the generation of waste heat is possible.

The temperature in technological processes of industrial production varies within a range wide enough, and, according to the temperature level, the waste heat can be conditionally classified into low-, medium- and high-temperature heat [2]. Within each temperature range, the application of this or that technology for the useful utilization of waste heat may have different efficiency. Utilization of high-temperature heat is the simplest way to proceed, both economically and technologically, while the beneficial application of low-temperature energy requires the use of more expensive technologies. It is possible to increase the energy efficiency of industrial enterprises by improving the technological process. In [3,4], a method for increasing the generation of synthesis gas due to co-pyrolysis and co-gasification of polypropylene and polystyrene is described.

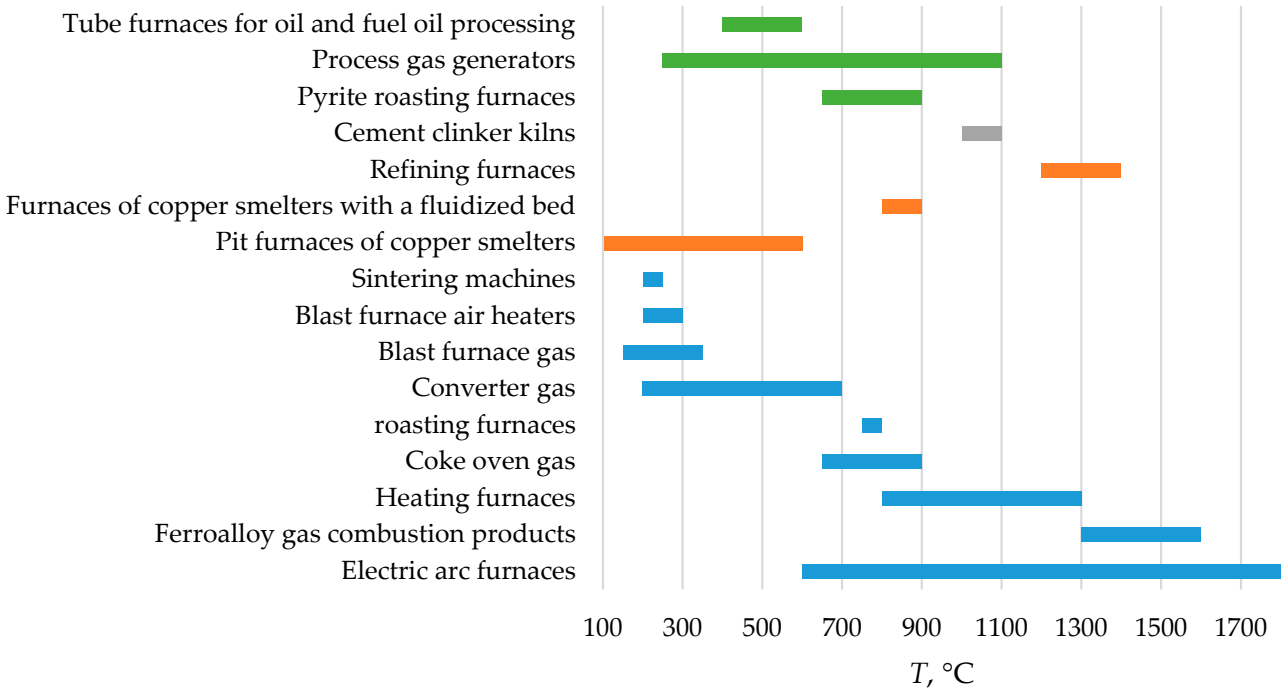


Figure 2. Temperature range of technological processes that may possibly generate the waste heat (based on [2,5,6]) (blue—metallurgy, orange—non-ferrous metallurgy, gray—cement manufactory, green—petrochemicals).

One of the actively developing areas of waste heat utilization in the industry is the production of electricity using power plants operating on the organic Rankine cycle (ORC). In the last decade, ORC has been actively applied to geothermal energy, as the use of an organic working fluid is more efficient for generating electric power based on low-temperature heat than steam. As of 2020, the total global installed capacity of ORC has already exceeded the value of 4000 MW, and the growth for the period from 2016 to 2020 has reached more than 40% [7]. Another actively developing area of ORC application is its use in industrial enterprises for the purpose of energy saving.

In the last 10 years, a relatively large number of projects using ORC plants at industrial enterprises have been implemented. Thus, Exergy (Olgiate Olona, Italy) was commissioned by Danieli Environment to design and install a 1.2 MW ORC plant at the Pozzuolo del Friuli steel plant in Italy. Extraction of heat from the electric arc furnace reduced CO_2 emissions by 2900 tons per year, and fuel consumption went down by 1500 tons of oil equivalent per year [8]. The need to use an ORC plant was justified by the growing cost of electricity in the region and the need to reduce the carbon intensity of the production. Also, Exergy installed ORC plants at the Şişecam glass factory (Targovishte, Bulgaria) in 2015: the total capacity of the units was 5 MW, the temperature of the circulating oil ranged from 150–300 °C, the reduction of carbon dioxide emissions was about 14,000 tons per year, and fuel consumption reduced by 7100 tons of oil equivalent per year. In 2020, a 3.5 MW plant was installed by Exergy at the CementiRossi cement plant (Pederobba, Italy) with an oil temperature ranging from 100–280 °C, a gross efficiency of 22.8%, and a cycle with intermediate freon superheating. The project was implemented with due account for the requirements for the use of non-combustible, fire-safe heat carriers.

Turboden (Brescia, Italy), a part of Mitsubishi Heavy Industries, develops and supplies ORC plants with electrical output of up to 20 MW for the geothermal power sector, industrial plants, incinerators, and other applications. A large number of ORC plants are manufactured by the company for biomass-based power generation, and the capacity of such plants usually does not exceed 5 MW. In the field of heat utilization, the largest number

of projects is heat utilization at cement plants (more than 16 projects), glass production (12 projects), and metallurgical plants (six projects).

Another actively developing trend is the use of ORC plants to utilize heat from flue gases in gas turbine units. In such binary cycles, the heat from the flue gases, instead of water vapor, vaporizes an organic heat carrier to produce additional electricity. Since 2008, Turboden has completed more than 16 projects to add ORC units with gas turbine plants. Currently, a 25 MW plant is under construction by Turboden to utilize the exhaust heat of GASCO's Dahshour gas compressor station (Dahshour, Egypt). The addition of ORC allows the generation of up to 40% of added power, with a net efficiency of the plants above 50% [9]. The potential of this area is also underlined by the fact that in 2019, Turboden and Siemens launched a joint Heat ReCycle project to produce combined cycle plants that use an organic Rankine cycle as the downstream cycle for highly efficient power generation with reduced CaPEX and OPEX, compared to a steam-water cycle [10].

Paper [11] reviews organic heat carriers for electric power generation on the basis of low- and middle-temperature heat sources. Criteria for the choice of the working fluid for the organic Rankine cycle were established: the selection shall take into account both the thermodynamic properties of the working bodies (their critical parameters and the shape of the saturation line curve) and the ecological parameters. Paper [12] contains an analysis of the productivity and optimization of the organic Rankine cycle for waste heat recovery. Paper [13] describes the research on cycles for the utilization of waste heat at a cement factory. A comparison of two technologies—steam-power cycle and ORC—showed that at gas temperatures above 310 °C, the ORC becomes less efficient than the steam-power cycle. Work [14] presents a study on working fluid selection for ORC used in engine waste heat recovery.

Another direction of active development today is the use of supercritical carbon dioxide in closed cycles for power generation. Critical parameters for carbon dioxide are 30.98 °C and 7.38 MPa. Thus, low-potential cycles with the use of carbon dioxide may be the Rankine cycles or the Brayton cycles, depending on the final pressure and temperature in the condenser. The use of the supercritical carbon dioxide cycles was considered as early as 1968 in a paper by the Italian scientist Angelino [15,16]. In his works, Angelino evaluated the efficiency of the Brayton carbon dioxide cycle with regeneration, pre-compression, re-compression, split expansion, partial cooling, and improved regeneration. The initial temperatures were taken as 500–800 °C. The same cycles were considered in the paper [17] at an initial temperature of 550 °C. Depending on the initial pressure, different cycles displayed the maximum efficiency. The paper [18] is dedicated to the analysis of the possibility of using carbon dioxide power cycles at thermal power plants. Brayton cycles with recompression at a sufficiently high initial temperature are capable of providing an increased level of energy efficiency in power generation. The carbon dioxide cycle has also been considered for the utilization of waste heat from a diesel gas piston generator [19].

Under conditions where the source temperature is high enough, e.g., in the case of gas turbine exhaust or cement clinker, more efficient cooling of the heat carrier can be achieved by using combined power cycles consisting of several independent circuits. Diagrams for the utilization of waste gas heat downstream of the gas turbine plant, in which the steam-power cycle and the organic Rankine cycle are arranged sequentially, are reviewed in the paper [20]. In such combined cycles, the final efficiency level exceeds that of twin-cycle steam turbine plants. The paper [21] reviews a combined cycle scheme for the utilization of gas turbine exhaust heat, including the Brayton recompression cycle using carbon dioxide and the Brayton cycle with partial heating.

Intensification of resource conservation and energy efficiency in energy-intensive industries, which has been observed in recent decades, predetermines the need to substantiate the feasibility of applying certain technical solutions for the useful utilization of waste heat for power generation. A comprehensive thermodynamic and economic scenario analysis is required to evaluate the efficiency of different layouts and heat carriers for utilization plants. The wide choice of possible options for the implementation of heat-utilizing plants makes it

necessary to develop recommendations for selecting layouts and working media depending on the operating conditions of the plants. This paper presents the results obtained during an analysis of the thermodynamic efficiency of technologies for utilizing secondary energy resources for power generation.

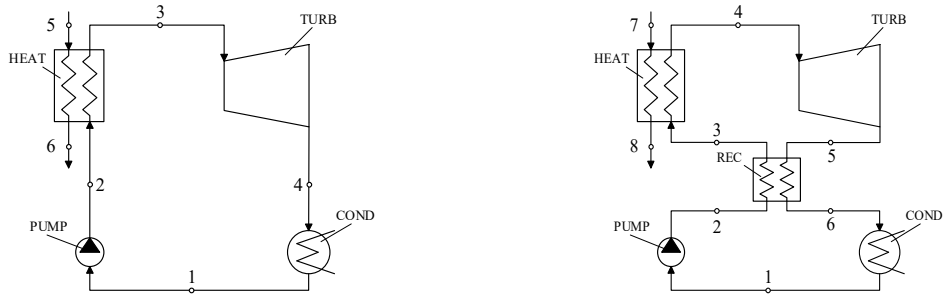
2. Object of the Study

This work considers options for the application of different working media and plant layouts for the utilization of waste heat. The most efficient existing and future plant layouts were chosen as the study objects:

1. Organic Rankine cycle;
2. Brayton cycle using supercritical carbon dioxide;
3. Water-steam Rankine cycle;
4. Combined cycles.

The choice of these plant layouts is justified by the fact that they are the most efficient options and are considered for power generation based on waste heat. The sequential utilization of heat in multiple cycles can provide efficient power generation, so the paper also considers the possibility of using a combination of multiple power cycles.

A diagram of the organic Rankine cycle for the utilization of waste heat is shown in Figure 3. The heat carrier from the thermal plant (waste heat source) transfers energy in the waste heat boiler (WHB) directly to the organic heat carrier (or intermediate thermal oil), after which it is cooled and carried away through the exhaust pipe to the atmosphere (or to the sewage system if the heat carrier is a liquid). An organic working fluid with a low boiling point in the liquid phase is compressed in the pump (process 1–2), heated in the WHB, vaporized, and then the steam is superheated (process 2–3). If the pressure of the compressed medium after the pump exceeds the critical pressure, the heating process takes place without an obvious phase transition. Once heated, the organic working fluid expands in the turbine, doing work (process 3–4), which in turn is transferred to the electric generator to generate electrical energy. The steam, after expansion, enters the condenser, where it is cooled and condensed (process 4–1), thus completing the cycle. An alternative plant layout is the use of a recuperator in which the steam expanded in the turbine transfers the residual heat energy to the working fluid compressed in the pump. This may ensure an increased level of energy efficiency for the plant; however, due to the increase in the temperature of the medium entering the WHB, the residual heat content of the medium entering the chimney will increase, while the depth of heat utilization in the system will be reduced. Both versions of the plant layout are reviewed in this paper, taking into account the possibility of applying sub- and trans-critical cycles.



(**a**) Rankine cycle (**b**) Rankine cycle with recuperator

Figure 3. Rankine cycle diagram for the utilization of waste heat.

The paper also considers a heat recovery diagram with the Brayton recompression cycle using supercritical carbon dioxide (Figure 4). There is no phase transition in such a cycle, and heat is supplied to carbon dioxide with parameters above the critical point (process 12–1). The heated gas expands in the turbine, performing work (process 1–2), releasing

residual heat in the high-temperature and low-temperature recuperators (processes 2–3, 3–4), and then splits into two streams (processes 4–5, 4–9). The first stream is cooled in the chiller to a near-critical temperature (process 5–6), then compressed in the main compressor (process 6–7) and heated in the low-temperature recuperator (process 7–8). The second stream is compressed in the recompression compressor (process 9–10) before being mixed with the first stream (processes 8–11, 10–11), after which the mixed stream is heated in the HTR (process 11–12) and enters the WHB.

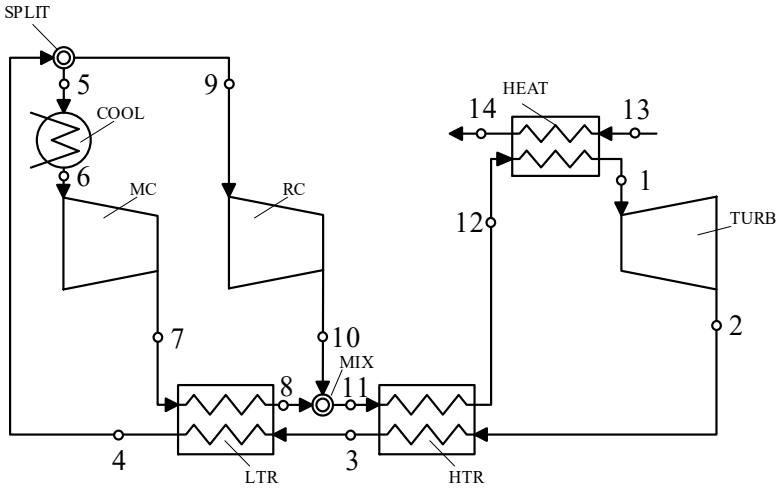
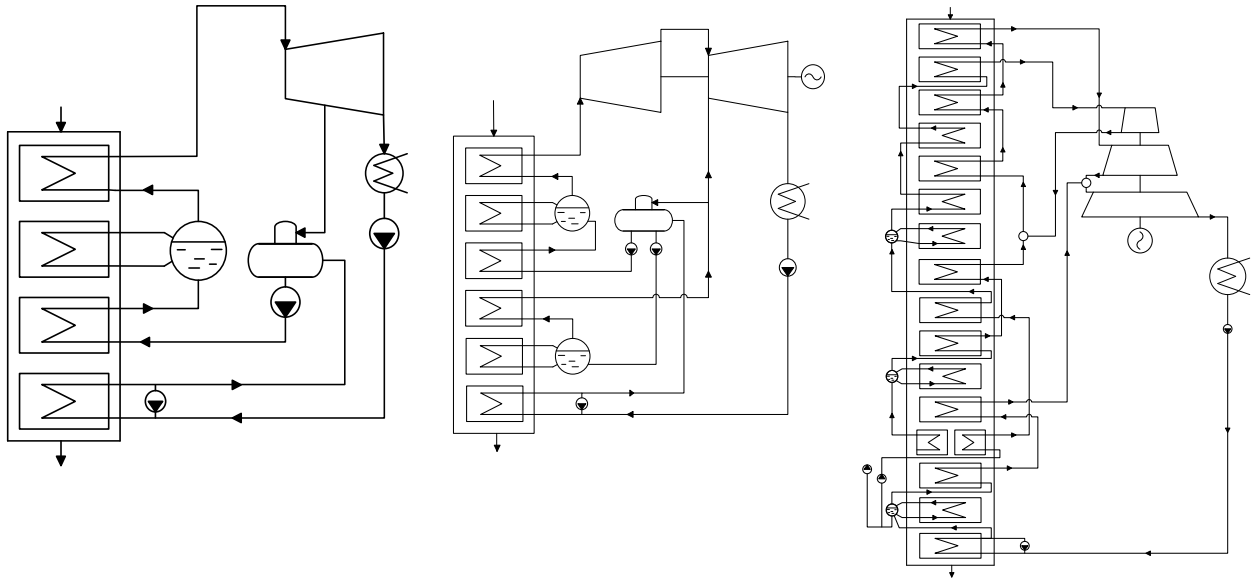


Figure 4. Schematic diagram of the Brayton recompression cycle for the utilization of waste heat.

With gas temperatures downstream of the waste heat source being above 400 °C, the most traditional solution is to use a water heat carrier. In such a diagram, the water is heated in the economizer and vaporized, after which the steam is superheated and delivered to the turbine, where it expands and works. The steam used enters the condenser, after which it is compressed in the pumps and transferred back to the WHB. Therein, it is possible to select the plant layout with one, two, and three pressure circuits (Figure 5).



(**a**) One pressure circuit (**b**) Two pressure circuits (**c**) Three pressure circuits

Figure 5. Steam-power cycle layouts for waste heat recovery.

The listed layout options are considered for electric power generation on the basis of waste heat from the furnace plant, whereby, for the purposes of comparison under

comparable conditions, the heat carrier is air. The initial air temperature varies within a wide range: it depends mainly on the processes occurring in the heating plant, plant design, and parameters. Therefore, this paper considers options within a wide range of initial temperatures.

3. Methods

The main research method in the present work is the mathematical modeling of thermodynamic cycles for the plants mentioned above. Energy efficiency during the useful utilization of waste heat can be estimated by the value of generated electric power, which will depend on the layout and parameters of the utilization unit and is a function of the heat source parameters: temperature, heat capacity, and mass flow rate of the heat carrier. With this in mind, this study evaluates specific performance (per unit mass flow rate of the cooled heat carrier) of utilization, with air considered as the heat carrier and the temperature corresponding to the temperature of waste heat.

The sequence of the study included the following main steps:

1. Calculation of thermodynamic cycles for the considered plants and optimization of their key parameters, determination of specific electric power and the degree of waste heat utilization;
2. Comparison of the specific capacity of plants and determination of the most efficient layouts and heat carriers for the given temperature range of the source;
3. Determination of the possibility of using thermodynamic cycles of combined installations and assessment of their energy efficiency.

In order to obtain a correct assessment of the prospective application of certain layout solutions, the cycle indicators are compared on the basis of the specific power of plants and their efficiency at different parameters of the waste heat source. In this case, a change in the initial temperature in a wide range will cause changes in the optimal ratio of the plant operating parameters (e.g., initial pressure). In this regard, for the correctness of the analysis, this paper includes parametric optimization of the previously listed plants in order to maximize their electrical power. Optimization was carried out by enumerating all possible combinations of parameters in cycles (in a limited range of parameter changes). The respective conditional block diagram is shown in Figure 6. After calculation, the processing of the results involved excluding the results that were unphysical or did not meet the requirements of the calculation. Table 1 summarizes the main parameters to be varied and their ranges of variation.

Table 1. Variable parameters in models.

Parameter P_i	P_{imin}	P_{imax}	P_{istep}
Gas temperature at the inlet to WHB, °C	150	700	50
Dimensionless mass flow rate of the working fluid in the cycle, kg/kg	0.1	5	0.1
Organic Rankine cycle			
Pressure after freon pump, MPa	1	30	1
Working fluid	R134a, R236ea, CO_2, R41, R124		
Recompression cycle			
Recompression ratio, %	50	100	5
Initial pressure, MPa	15	35	1
Steam turbine unit			
Primary circuit pressure, MPa	1	15	15
Secondary circuit pressure, MPa	1	15	15
Third circuit pressure, MPa	0,1	10	10

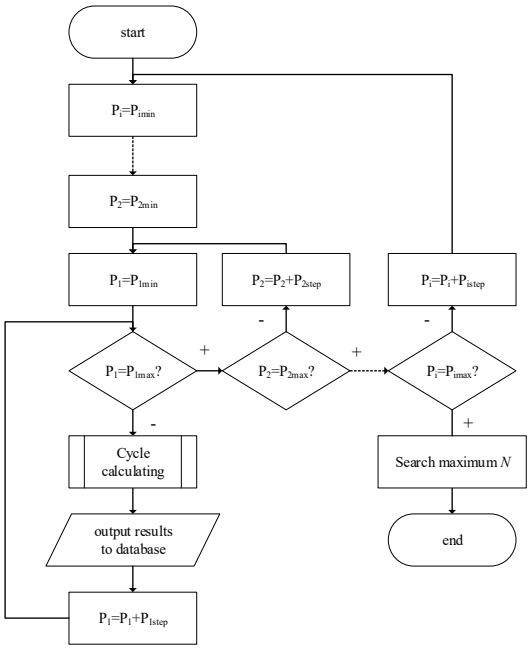


Figure 6. Block diagram of parametric cycle optimization.

The calculation of cycles was based on the compilation of a system of equations describing thermodynamic processes in the main elements of the cycle and their combined solution. The NIST REFPROP database was used to determine the thermal and physical properties of working bodies. The main equations used in the calculations are presented below.

The compression and expansion processes in pumps, compressors, and turbines were calculated with a constant coefficient of relative internal (isentropic) efficiency. The mass enthalpy of the working fluid as a result of compression was calculated as:

$$h_{c.out} = h_{c.in} + \left(h'_{c.out} - h_{c.in}\right)/\eta_c \quad (1)$$

where $h_{c.in}$—mass enthalpy of the working fluid at the compressor/pump inlet, kJ/kg;

$h'_{c.out}$—theoretical mass enthalpy of the working fluid caused by isentropic compression, kJ/kg;

η_c—compressor/pump isentropic efficiency factor.

Mass enthalpy of the working fluid after expansion in the turbine was calculated by the formula:

$$h_{t.out} = h_{t.in} - \left(h_{t.in} - h'_{t.out}\right) \times \eta_t \quad (2)$$

where $h_{t.in}$—mass enthalpy of the working fluid at the turbine outlet, kJ/kg;

$h'_{t.out}$—theoretical mass enthalpy of the working fluid caused by isentropic expansion, kJ/kg;

η_t—turbine isentropic efficiency factor.

The calculation of heat exchangers (WHB sections and recuperators) is based on the heat balance equation:

$$G_h \times (h_{h.in} - h_{h.out}) \times \varphi = G_c \times (h_{c.out} - h_{c.in}) \quad (3)$$

where G_h and G_c—mass flow rate of the hot and cold working fluid accordingly, kg/s;

$h_{h.in}$ and $h_{c.in}$—mass enthalpy of the hot and cold working fluid at the heat exchanger inlet, kJ/kg;

$h_{h.out}$ and $h_{c.out}$—mass enthalpy of the hot and cold working fluid at the heat exchanger outlet, kJ/kg;

φ—heat loss factor.

The calculation of heat exchangers is based on an iterative search for the mass enthalpy of one of the flows at the heat exchanger outlet, at which the minimum temperature difference in the case of countercurrent flow of media will be equal to a pre-defined value.

The internal capacity of turbines, pumps, and compressors was calculated as follows:

$$N = G_{in} \times (h_{out} - h_{in}) \quad (4)$$

where G_{in}—mass flow rate of the working fluid, kg/s;

h_{in} and h_{out}—mass enthalpy of the working fluid at the inlet and outlet of turbine, pump, or compressor, kJ/kg.

The net specific electrical power of the plant was calculated by the formula:

$$N_{net} = \sum N_t \times \eta_m \times \eta_e - \sum \frac{N_c}{\eta_m \times \eta_e} \quad (5)$$

where

N_t and N_c—internal power of turbines and compressors/pumps, kW;

η_m and η_e—efficiency factor of mechanical transmission and electric generator/motor.

The energy efficiency of waste heat utilization was determined as follows:

$$\eta = \frac{N_{net}}{h_{g.in} - h_{g.out}} \quad (6)$$

where $h_{g.in}$ and $h_{g.out}$—mass enthalpy of gases at the inlet and outlet of the WHB, kJ/kg.

The flow mixing process was also calculated based on heat and material balances.

The main constants used in the calculations are presented in Table 2.

Table 2. Constants in mathematical models.

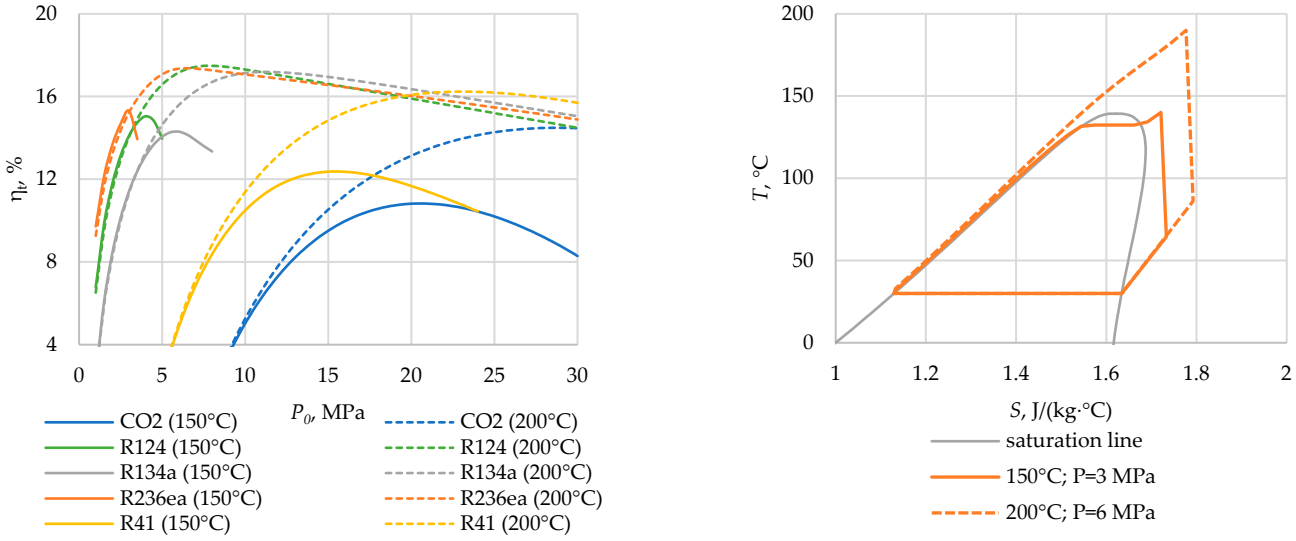
Parameter	Value
General constants	
Hot heat carrier	Air
Hot heat carrier flow rate, kg/s	1
Hot heat carrier pressure, MPa	0.1
Minimum temperature difference in the WHB, °C	10
Minimum temperature difference in the recuperators, °C	5
Temperature at the cold source of the cycle (condenser, cooler), °C	30 32 for S–CO_2
Efficiency of mechanical transmission, %	99
Efficiency of electric generator/motor, %	99
Minimal quality of working fluid in the turbine, %	90
ORC	
Isentropic efficiency of turbines, %	85
Isentropic efficiency of pumps, %	80
Recompression cycle	
Isentropic efficiency of turbines, %	90
Isentropic efficiency of compressors, %	85
STU	
Water underheating to boiling temperatures in economizers, °C	10
Water heating in the deaerator, °C	10
Pressure in the deaerator, MPa	0.12
HPC efficiency	0.87
MPC efficiency	0.9
LPC efficiency	0.85

4. Results and Discussion

4.1. Organic Rankine Cycles for Waste Heat Recovery

Electric power generation with Rankine cycle power units using organic media with low critical parameters as a working fluid is an effective solution when the temperature and capacity of the waste heat source are low.

The final efficiency level of such plants will be largely influenced by both the heat supply conditions and the choice of the power cycle working fluid and the main equipment parameters. Figure 7a presents a graph showing the dependence of the net efficiency of the simple organic Rankine cycle on the pressure downstream of the pump P_0 and the type of working fluid at the inlet air temperature of 150 °C and 200 °C. For all calculated cases, the pressure after expansion in the turbine was selected so that the condensation temperature was 30 °C, which corresponds to the typical value for thermal power plants under conditions of power cycle cooling by water (or when using air condensers with an outside air temperature not exceeding 25 °C).



(**a**) $\eta(P_0)$ (**b**) R236ea T–S diagram

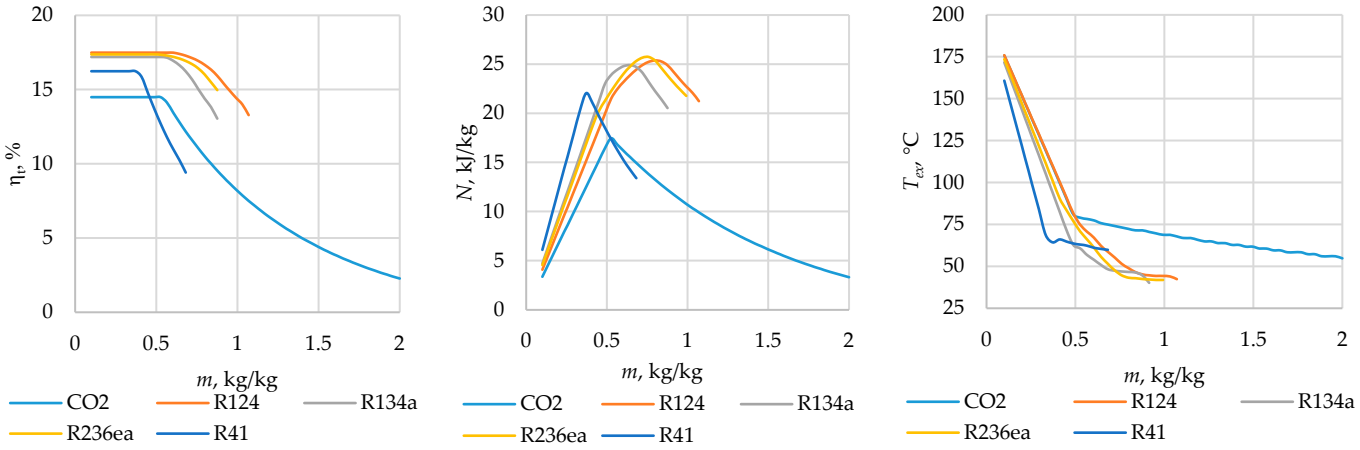
Figure 7. Dependence of the net efficiency of the CRO on the initial pressure and the type of working fluid (solid line—$T_{g.in}$ = 150 °C, dashed line—$T_{g.in}$ = 200 °C).

Similar to the conventional Rankine steam-water cycle, the net efficiency depends largely on the initial pressure: on one side, it defines the final pressure drop during expansion in the turbine, which determines the final useful work and also affects the energy required for compression in the pump. Under conditions of heat supply to the cycle at a sufficiently high temperature of the utilized source, it is possible to carry out the cycle at supercritical parameters: in this case, heating of the organic working fluid will occur without a pronounced phase transition, which will allow the cycle to increase the average integral temperature of heat supplied to the power cycle (Figure 7b).

The thermal and physical properties of organic working bodies (their critical parameters and the shape of the saturation curve) will largely determine the maximum permissible efficiency of the power cycle. It can be seen that at a gas temperature of 150 °C, the highest efficiency is achieved when freon R236ea with an initial pressure of about 3 MPa (η = 15.3%) is used as a working fluid, while the maximum efficiency of the cycle using freon R124, equal to 15.0%, is achieved at a pressure of 4 MPa. As the initial temperature increases, both the power cycle efficiency level (η_{R236ea} = 17.4%, η_{R124} = 17.5%) and the optimal initial pressure ($P_{0,R236ea}$ = 6.5 MPa, $P_{0,R124}$ = 8.0 MPa) increase.

It should be noted that when utilizing the heat of gases emitted from the heating plant, the final level of electric power generated by the power cycle will be defined not only by

the choice of optimal parameters from the point of view of maximizing efficiency but also by the degree of gas cooling, which determines the total amount of heat energy supplied. Analyzing the WHB heat balance, one can easily find that under the conditions of a limited minimum temperature difference on the heat transfer surfaces, the degree of gas cooling will be determined mainly by the mass flow rate of the working fluid in the power cycle. With its increase, on one side, the amount of heat energy taken from gases will increase and, on the other side, the heating of the working medium in the power cycle will be reduced. Figure 8 shows graphs displaying the dependence of the ORC net efficiency, its specific electric power (power at gas flow m_g = 1 kg/s), and gas temperature at the WHB outlet on the dimensionless ratio of the cycle working fluid mass flow rate to the gas flow rate (mass flow ratio), with the initial pressure at each point being optimized. The dependence shows that at sufficiently small values of the flow rates ratio, the change in this value does not lead to a change in the cycle efficiency: the thermal energy of gases is sufficient for the maximum possible heating of the working fluid, subject to a temperature drop limitation on the WHB heat transfer surfaces. With the increase of m up to a critical ratio of mass flow rates m^*, specific electric power grows practically linearly due to the increase of heat perceived by the cycle without changes in thermodynamic parameters; however, at values $m > m^*$, the thermal energy of gases becomes insufficient to ensure the high temperature of working fluid upstream of the turbine, while the saturation pressure necessary for the implementation of the thermodynamic cycle goes below optimal. This results in a dramatic reduction in both the net efficiency of the power cycle and its specific electrical power.



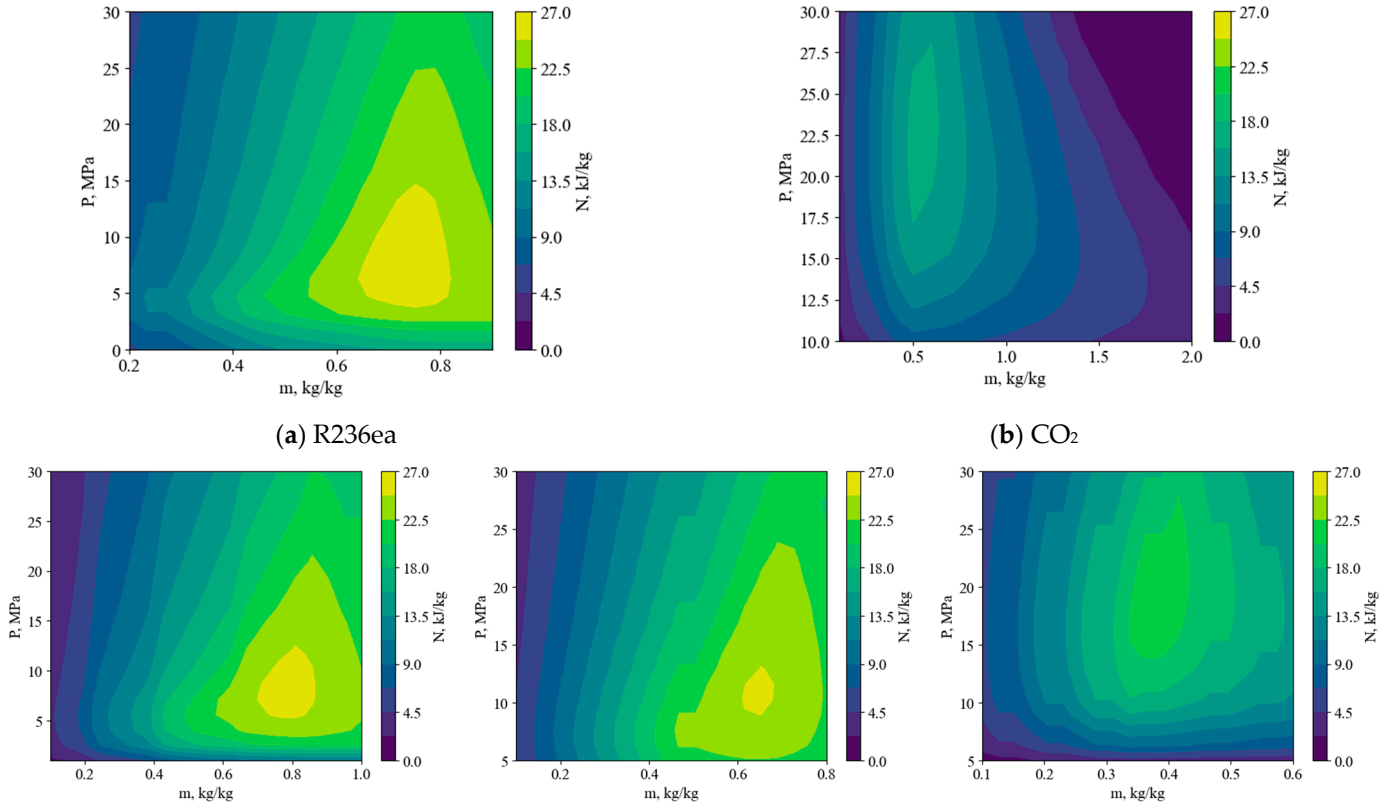
(**a**) $\eta(m)$ (**b**) $N(m)$ (**c**) $T_{ex}(m)$

Figure 8. Dependence of net efficiency (**a**), specific electric power (**b**), and gas temperature downstream of WHB (**c**) on the working fluid flow rate in the power cycle $T_{g.in}$ = 200 °C.

The maximum ORC electrical power will be achieved by ensuring the mass flow rate of the working fluid at which the critical value of the mass flow rate ratio m^* is reached. Simultaneously, it will depend on the thermal and physical properties of the organic working fluid and pressure in the cycle. Figure 9 shows the results of optimizing the ORC thermodynamic parameters with the temperature of gases at the WHB inlet $T_{g.in}$ = 200 °C. The contours show that a multi-parameter cycle optimization is required to achieve maximum useful power for waste heat recovery.

Results from comparing the efficiency and power of cycles with different working bodies (Figure 10) show that the choice of working fluid will be determined, among other things, by the choice of the target function: at $T_{g.in}$ = 150 °C, in the case of maximizing the thermal efficiency, freon R236ea should be chosen, and in the case of maximizing the electrical power—R134a. With the increase in gas temperature at the WHB inlet, R236ea at $T_{g.in}$ = 200 °C and R124 at $T_{g.in}$ = 250 °C become the optimal (with capacity as a target function) working fluid. It should be noted that considering the net efficiency index as

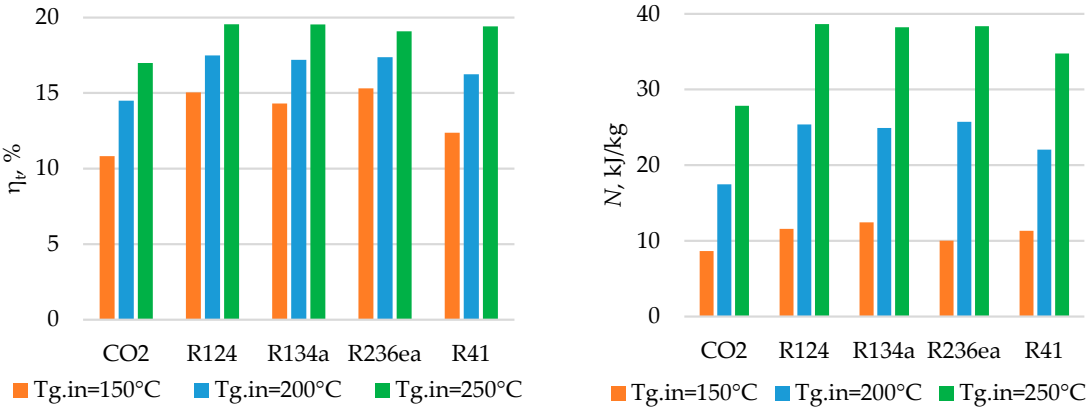
a target function for optimization of the power cycle thermodynamic parameters is not always reasonable: this value represents the efficiency of supplied heat utilization without taking into account the heat carried away by gases after the WHB. Electrical power, in turn, will be determined not only by the efficiency of the circuit but also by the possible degree of gas cooling.



(**a**) R236ea (**b**) CO_2

(**c**) R124 (**d**) R134a (**e**) R41

Figure 9. Contour of ORC-specific power when using different working bodies.

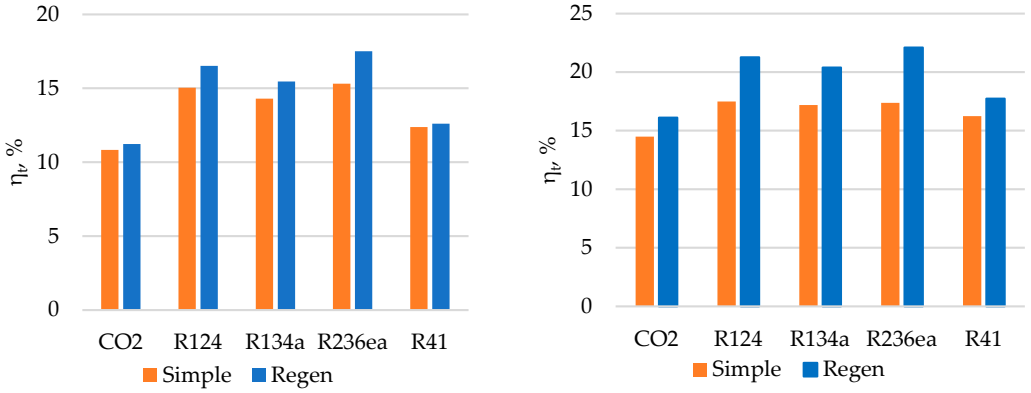


(**a**) Thermal efficiency (**b**) Specific electric power

Figure 10. Comparison of net efficiency and ORC capacity using different working bodies.

Due to the low critical parameters of organic working bodies and the shape of the phase equilibrium curve defined by expansion in the turbine, the medium can remain in the state of superheated steam (without moisture), which makes it possible to apply the plant layout with residual heat recovery for preheating the working fluid upstream of

WHB. This makes it possible to increase the net cycle efficiency while the effect of heat recovery increases with the increase of the gas temperature at the WHB inlet. Thus, at an inlet gas temperature of $T_{g.in}$ = 150 °C, the absolute increase of η can be 0.2–2.2%, and at 200 °C—1.5–4.7% (Figure 11). The efficiency increase is achieved by increasing the working medium temperature upstream of the WHB (increasing the average integral temperature of the heat supply) and reducing the heat dissipated in the condenser due to heat recovery. On the other hand, heat recovery limits the cooling of flue gases and, consequently, the amount of heat supplied to the cycle.



(**a**) $T_{g.in}$ = 150 °C (**b**) $T_{g.in}$ = 200 °C

Figure 11. Comparison of net efficiency for the simple and regenerative ORC.

In this connection, the analysis of power cycles for the utilization of the gas heat shall be performed with due account of the degree of cooling: depending on the chemical composition of gases, there can be requirements for the minimum WHB temperature. Most often, such requirements are based on the avoidance of condensate precipitation due to reaching the dew point: depending on the source of waste heat, it is possible that water, various acids, and solid precipitates may be released in the gas medium, which will lead to corrosion and subsequent destruction of the WHB heat-exchange surfaces and other structural elements.

Figure 12 shows the field of points for the possible implementation of the power cycle, where the *X*-axis indicates the temperature of flue gases downstream of the WHB, and the *Y*-axis indicates the specific electric power of the ORC with carbon dioxide as a working fluid. At a fixed mass flow rate, a change in cycle pressure leads to a change in both cycle power and flue gas temperature: a maximum can be seen in the $N(T_{ex})$ coordinates that is reached when the optimum pressure is used downstream of the pump. A change in flow rate, in turn, leads to a change in the flue gas temperature and electrical power according to the earlier described relationships so that both P_0 and m affect N and T_{ex}. Taking into account the flue gas temperature limitations, it is most appropriate to choose a set of parameters at which the maximum N is achieved at a given limit T_{ex}. Analyzing the $N(T_{ex})$ diagram, one can see that the maximum power at a given flue gas temperature is not always achieved at the optimal pressure: it is possible to run a cycle with a higher mass flow rate but at a non-optimized pressure, in which case the electrical power will be higher than in the optimized version. At $m > m^*$, the optimal solution is to overestimate the mass flow rate under reduced pressure, while at $m < m^*$, the optimal solution is to overestimate the mass flow rate with overpressure. The green line in the diagram corresponds to the pressure-optimized variant, and the blue line corresponds to the best optimization in terms of two target functions: electric power and flue gas temperature (Pareto optimization). It can be seen that the Pareto optimization will provide more electrical power for a given T_{ex} than the initial pressure optimization.

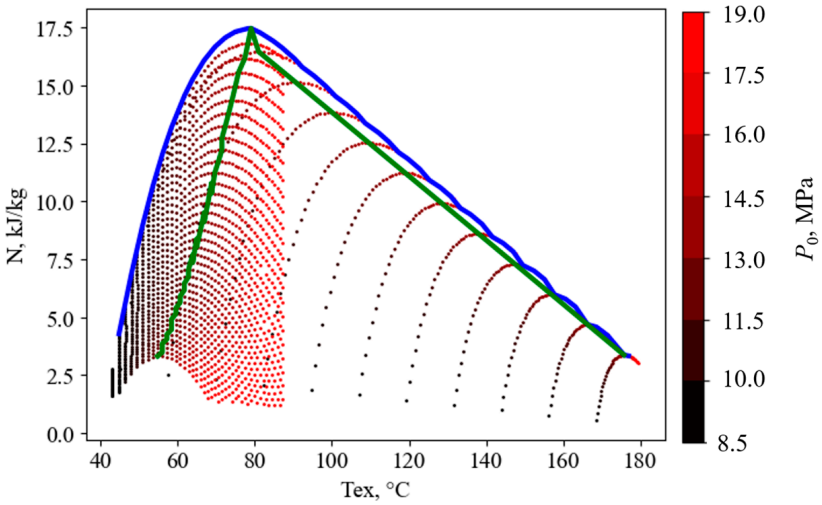


Figure 12. $N(T_{ex})$ diagram for ORC using CO_2 at T = 200 °C (green line—optimal pressure, blue line—Pareto solution).

Based on the results of parameter optimization, a series of $N(T_{ex})$ curve families were obtained for simple and recuperative ORC. Figure 13 shows that heat recovery in the cycle ensures the achievement of maximum power at higher T_{ex}, at the same time, as the initial temperature of gases at the WHB inlet increases, both maximum specific electric power of the cycle and T_{ex} value at which the maximum is achieved also increase.

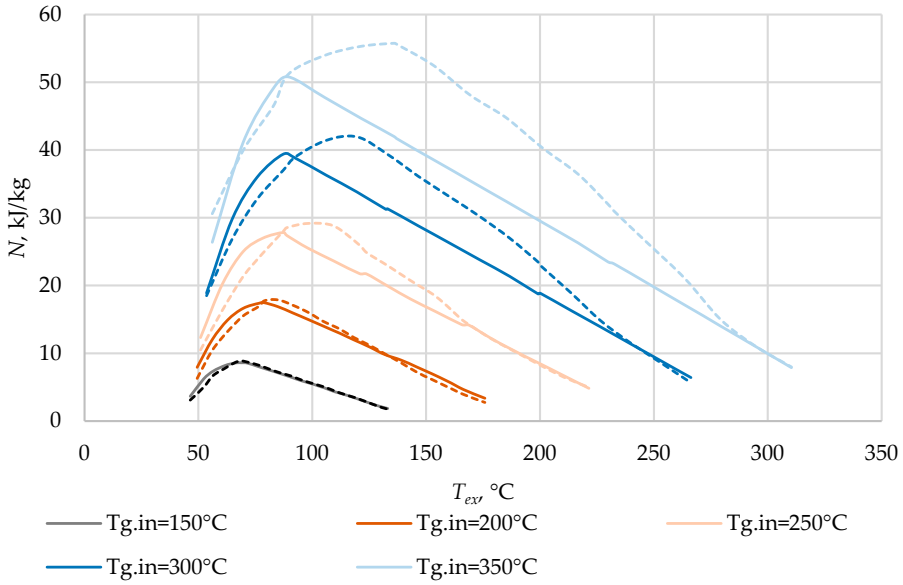


Figure 13. Dependence $N(T_{ex})$ for simple and regenerative ORC on CO_2 (solid line—simple cycle, dashed line—with recuperator).

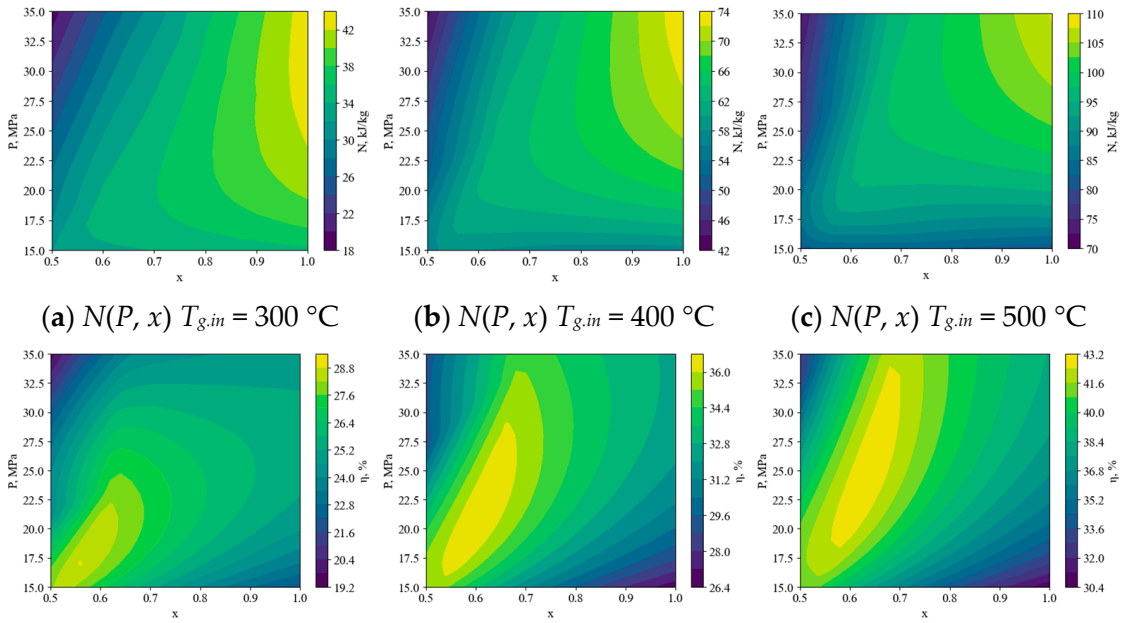
Thus, the use of organic Rankine cycles for waste heat utilization may be promising in conditions where the temperature of the heat source is relatively low: at higher initial temperatures, a transition to steam-power cycles, as well as to cycles with supercritical parameters, is possible.

4.2. Brayton Supercritical Carbon Dioxide Cycles

Compared to cycles using organic working bodies, the supercritical Rankine cycle using carbon dioxide has comparatively lower efficiency and power. However, a low critical temperature of CO_2, equal to T_c = 32 °C, makes it possible to create a closed Brayton cycle

with supercritical parameters in both the WHB and in the cold source of the cycle, while the efficiency of such a plant will be comparable to Rankine cycles since the cold source temperature will be at the same level. Unlike the cycle with condensation of the working fluid, in the case of cooling the supercritical medium with its subsequent compression, the temperature of the compressed medium will be high enough, which in turn will limit the heat recovery and the degree of WHB flue gas cooling. Adding recompression to the power cycle will result in an additional increase in the temperature of the working fluid at the WHB inlet, which will ultimately affect both the electrical output of the cycle and the net efficiency.

Figure 14 presents the power and efficiency contours of the Brayton recompression cycle from the initial cycle pressure and the fraction of recompression. Should the net electrical power of the power cycle be taken as a target function, it becomes obvious that the most efficient solution is the use of the regenerative rather than the recompression Brayton cycle, since practically at any value of the initial pressure, the cycle power (at the optimum mass flow rate) has a maximum at $x = 1$, i.e., when the entire carbon dioxide flow enters the main compressor. In turn, net efficiency, unlike power, has an extremum reached, which depends on P, at values $x = [0.5; 0.7]$, which is explained by maximizing the degree of heat recovery in HTR and LTR. Therefore, adding the recompression to the Brayton cycle may be appropriate under conditions where deep cooling of gases is not allowed.



(**a**) $N(P, x)$ $T_{g.in}$ = 300 °C (**b**) $N(P, x)$ $T_{g.in}$ = 400 °C (**c**) $N(P, x)$ $T_{g.in}$ = 500 °C

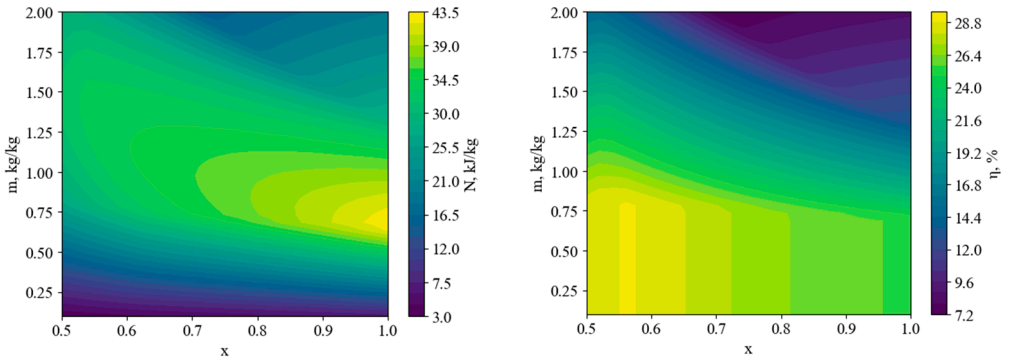
(**d**) $\eta(P, x)$ $T_{g.in}$ = 300 °C (**e**) $\eta(P, x)$ $T_{g.in}$ = 400 °C (**f**) $\eta(P, x)$ $T_{g.in}$ = 500 °C

Figure 14. Dependence of power and net efficiency of the Brayton cycle using S–CO_2 on initial pressure and fraction of recompression.

Figure 15 shows that, similar to Rankine cycles, in the recompression/recovery Brighton cycle, the ratio of the mass flow rates of the heat source and the working fluid of the cycle is a factor that largely determines the net electric power value of the power cycle. Thus, at a relative flow rate below the critical m^*, the specific power grows almost linearly with the increase in m, while η has maximum values and does not depend on m. At $m > m^*$, in the recuperative cycle, there is a reduction of electric power with the growth of m, and in the recompression cycle, the power growth slows down, followed by reaching a local maximum and dropping N.

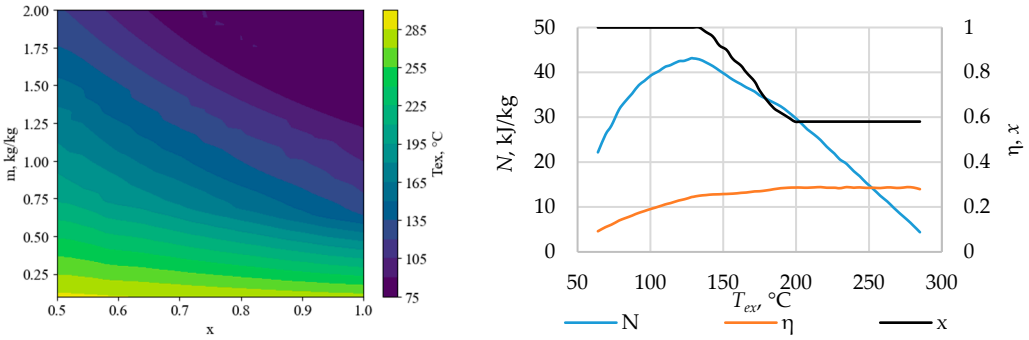
The achievement of higher specific electric power in the recuperative cycle in comparison with the recompression cycle is caused by different degrees of gas cooling: Figure 16a demonstrates that an increase in the recompression share in the cycle in the whole range of

m values leads to a decrease in temperature of flue gases downstream of the WHB. Under conditions where the depth of gas cooling is limited by environmental requirements, boiler operating requirements, or process requirements, simultaneous consideration of the cooling degree with the maximization of electrical output becomes necessary. $N(T_{ex})$ diagram presented in Figure 16b demonstrates that at $m < m^*$, the decrease in the temperature of flue gases occurs at η = const, while the virtually linear increase in the specific electric power of the cycle occurs only due to an increase in m at fixed thermodynamic parameters in the power cycle nodes (P, x). Further growth of electric power with a reduction in T_{ex} can be achieved by selecting suboptimal parameters from the efficiency point of view: an increase in the recompression share in the cycle leads to a reduction in HTR power and, as a consequence, to a reduction in the heat recuperation degree in the cycle and a reduction in the working medium temperature at the WHB inlet. In this case, a drop of η is observed, causing a slow growth of N: the first bend is observed on the graph of $N(T_{ex})$. Upon reaching the degree of recuperation $x = 1$, the electric power comes to its maximum, and it becomes possible to further reduce the temperature of flue gases by increasing the flow rate while reducing the initial pressure in the cycle along with a significant drop in efficiency and power.



(**a**) $N(m, x)$ $T_{g.in}$ = 300 °C (**b**) $\eta(m, x)$ $T_{g.in}$ = 300 °C

Figure 15. Dependence of power and net efficiency of the Brayton cycle using S–CO_2 on the mass flow rate and degree of recuperation.

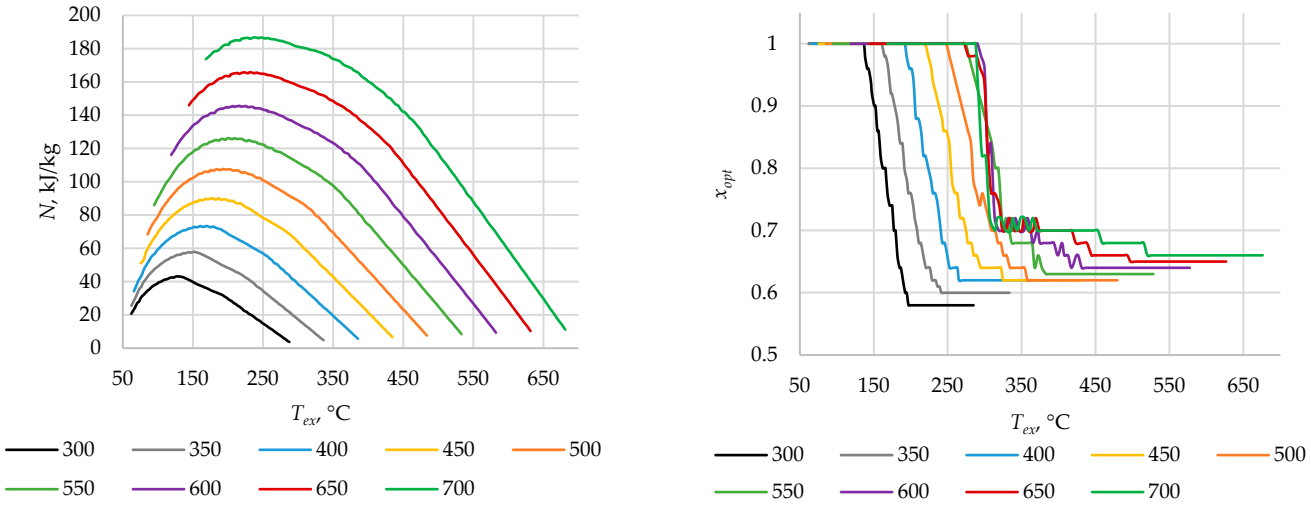


(**a**) (**b**)

Figure 16. The dependence of the exhaust gas temperature on the relative mass flow rate and recompression distance (**a**) and the dependence of the maximum specific electric power, net efficiency, and the optimal proportion of recompression on the exhaust gas temperature (**b**).

Figure 17 illustrates the dependence of maximum specific electric power and fraction of recompression, at which the maximum is reached, on the temperature of gases downstream of the WHB. It can be seen that regardless of the temperature of gases at the boiler inlet, the function $N(T_{ex})$ has both a maximum and a bend, while the values of characteristic

T_{ex} are also increasing with the increase of $T_{g.in}$. At the same time, the optimal value of recompression fraction grows at subcritical specific mass flow rates.



(**a**) $N(T_{ex})$ (**b**) $x_{opt}(T_{ex})$

Figure 17. The dependence of the maximum specific electric power (**a**) and the proportion of recompression (**b**), at which the maximum is reached, on the temperature of the gases after the recovery boiler.

Therefore, supercritical carbon dioxide cycles may be used for waste heat utilization under conditions where the heat source temperature is high and deep cooling of gases is inadmissible due to possible precipitation of condensate. If there are no such constraints, the Brayton recuperative cycle will generate more electrical power due to the ability to cool the source more intensively.

4.3. Steam-Power Cycles for Waste Heat Utilization

The use of water and water vapor for the production of electrical energy is a traditional solution at thermal power plants. In cases where the heat energy source is gases from the exhaust of a gas turbine plant or gases generated by a high-temperature heating plant, steam turbine plants with WHBs are used. The steam turbine plant, in this case, is most often designed without a developed system of regenerative feed water heating, and the design of the boilers provides for several pressure circuits (usually not more than 3) for deep cooling of gases.

Figure 18 compares the specific electrical power of a steam turbine plant with one, two, and three pressure circuits. At $T_{g.in}$ < 400 °C, the application of a cycle at three pressures has no practical sense, as the level of its efficiency will be comparable to that of the two-circuit cycle. On average, the two-pressure layout is found to be 8.8 kJ/kg more efficient than the single-pressure option, and the three-pressure layout is 20 kJ/kg more efficient.

In this case, the main reason for the increase in specific power of the steam-power cycle is the deeper cooling of gases in low-pressure circuits: this increases the total amount of thermal energy contributed to the cycle. Figure 19 shows the $N(T_{ex})$ diagram for steam turbine plants with one, two, and three pressures. It can be seen that two- and three-circuit units can be effectively used only in the case of deep cooling of gases: depending on $T_{g.in}$, the temperature of effective transition from a single-circuit to a two-circuit option is 140–170 °C, and the transition to a three-circuit option becomes practical when it is possible to cool gases down to temperatures of 100–110 °C. The graphs demonstrate that in layouts with one pressure circuit, more efficient electric power generation is possible at the same temperature of gases downstream of the WHB T_{ex} under conditions where $m < m^*$: specific electric power is higher than that in two- and three-circuit plant layouts.

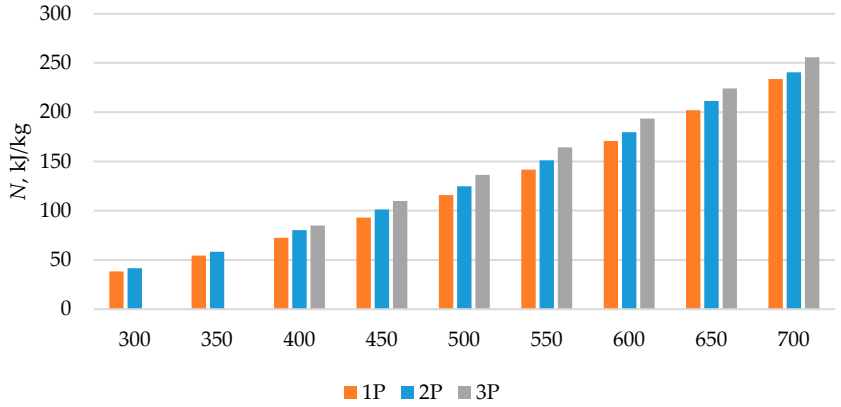


Figure 18. Comparison of maximum specific electric power of steam-power cycles at different temperatures of gases at the WHB inlet.

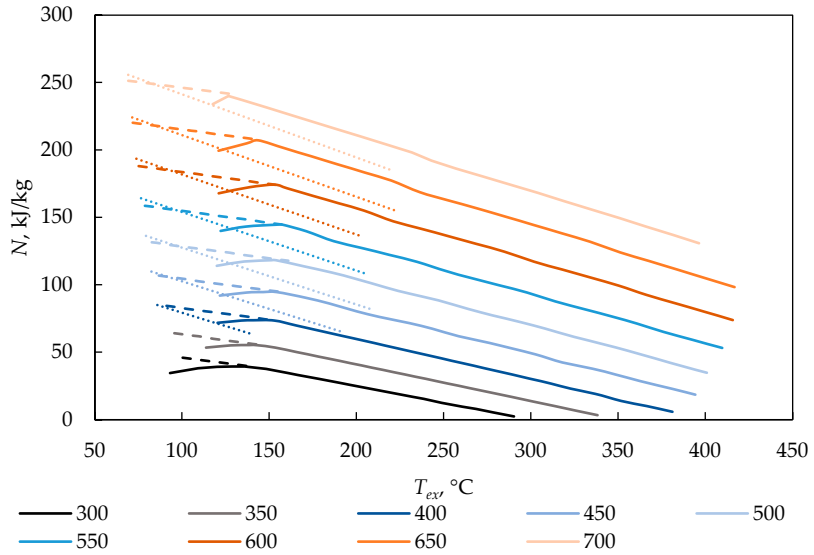


Figure 19. Dependence $N(T_{ex})$ for steam power cycles on one, two, and three pressure circuits (solid line—one contour, dotted line—two contours, dots—three contours).

In multi-circuit systems, water in the low-temperature region is vaporized at low pressures, which allows to cool the gases more intensively. It is known that the use of organic Rankine cycles can be more efficient under these conditions, which makes the possibility of combining steam-powered cycles with an ORC quite promising.

4.4. Sequential Heat Recovery in Several Power Cycles

Combined use of several heat recovery cycles may be promising under conditions where the waste heat temperature is high enough. In the case of sequential heat utilization in the high-temperature part, it is advisable to use circuits with a developed regeneration system that increases the internal efficiency of the cycle with a simultaneous increase in the residual heat content in the gases utilized in the second cycle. For example, the combined use of a Brayton recompression cycle with an organic Rankine cycle or a single-pressure steam turbine with the ORC can become efficient. Efficient heat distribution of flue gases between the high and low-temperature cycles is an important issue for such combined plants.

Figure 20 presents a graph demonstrating the dependence of specific electric power of the combined cycle, consisting of the recompression Brayton cycle using supercritical carbon dioxide and the organic Rankine cycle using R236ea, on the fraction of heat supplied to the Brayton cycle from the total heat. It can be seen that there is an optimal distribution

between the two circuits that provides the maximum sum of powers for the two cycles: as the share of the high-temperature cycle increases, its electrical power grows according to the dependence described in Section 4.2, while the power of the low-temperature cycle drops according to the dependence in Section 4.1. It can be seen from the graph that the maximum total power is reached when $m > m^*$ in the recompression cycle, but the maximum specific electrical power of the carbon dioxide cycle has not yet been reached. Therefore, the issue of heat distribution optimization is the key point for combined cycles.

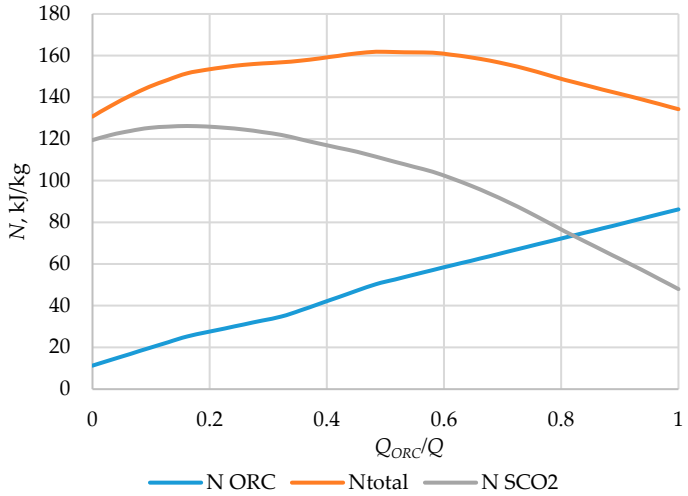
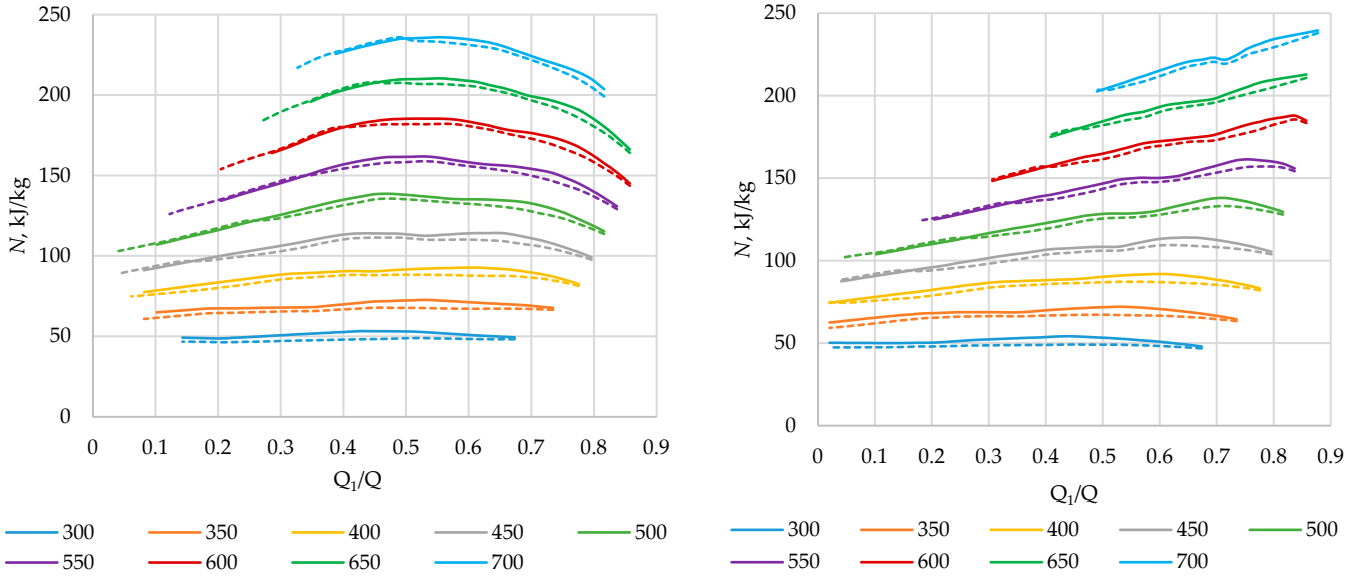


Figure 20. Dependence of the specific electric power of the combined cycle and its components on the distribution of thermal energy of gases.

Figure 21 compares the power of several combined cycles: a recompression cycle with simple and regenerative ORC and a single-circuit steam-power cycle with simple and regenerative ORC. The graphs demonstrate that practically, in the whole considered range of $T_{g.in}$, the highest values of specific electric power are achieved when using regenerative ORC in the low-temperature part. This is explained by the fact that when flue gases are cooled down to a temperature of 80 °C, heat recovery in the cycle practically does not cause any reduction in the electrical power of the ORC. It should also be noted that in contrast to the case of the recompression cycle applied in combination; there is no optimal heat distribution during the use of the steam-power cycle at $T_{g.in} > 600$ °C, which indicates that at such parameters, the traditional three-circuit steam turbine plant becomes more efficient.

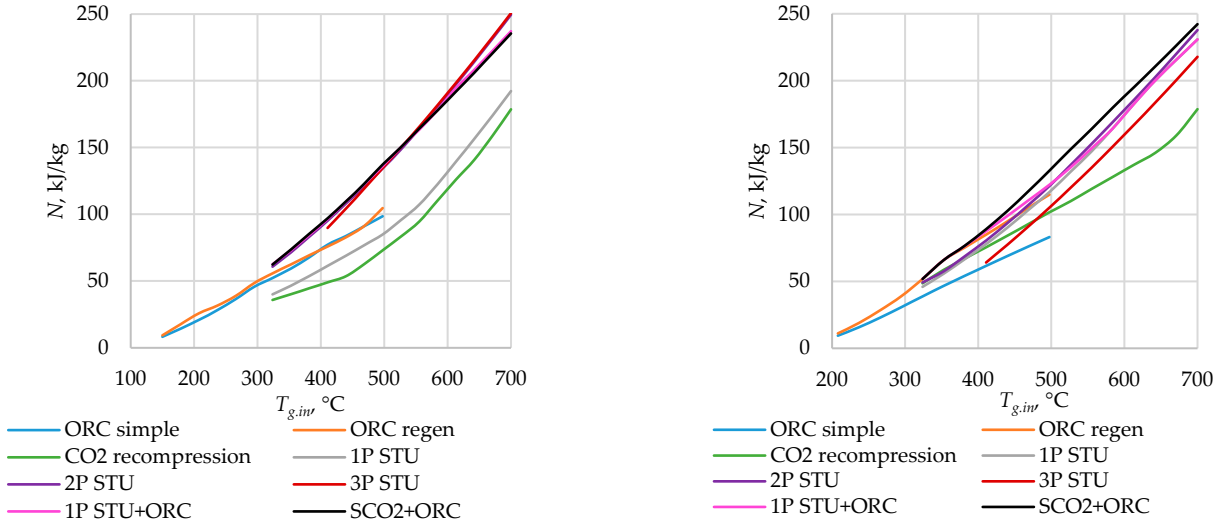
The obtained results are valid under the condition of cooling the gases to a temperature of 80 °C, which is a typical value at thermal power plants with combined-cycle gas turbines, where the excess air in the combustion products of the gas turbine is quite high. If the excess air in the combustion products is not large, and acid precipitation is possible in the combustion products, the minimum temperature of the gases after passing the heat exchange surfaces of the waste heat boiler will be higher. For example, at coal-fired power plants, the temperature of the combustion products at the inlet to the chimney may exceed 150 °C. This, in turn, will lead to a change in the energy indicators of the power cycles.

Figure 22 shows the dependence of the specific power of the power cycles considered in this paper on the temperature of the gases at the inlet to the waste heat boiler. In the case of limiting the minimum gas temperature to a level not lower than 80 °C with a boiler inlet gas temperature of up to 300 °C, the highest power is achieved using an organic Rankine cycle with a recuperator. At higher temperatures, steam-power cycles with two pressure circuits become more efficient, and at $T_{g.in} > 550$ °C—with three. Under conditions when the minimum gas temperature after the boiler should not be lower than $T_{ex} = 150$ °C, the use of combined cycles may become advisable: at temperatures above 400 °C, the specific electrical power of a combination of recompression and organic cycles becomes the highest among all those considered.



(**a**) SCO_2 + ORC (**b**) 1P STU + ORC

Figure 21. Dependence of combined cycle-specific power on heat distribution between cycles (solid line—ORC with recuperator, dotted dashed line—simple ORC).

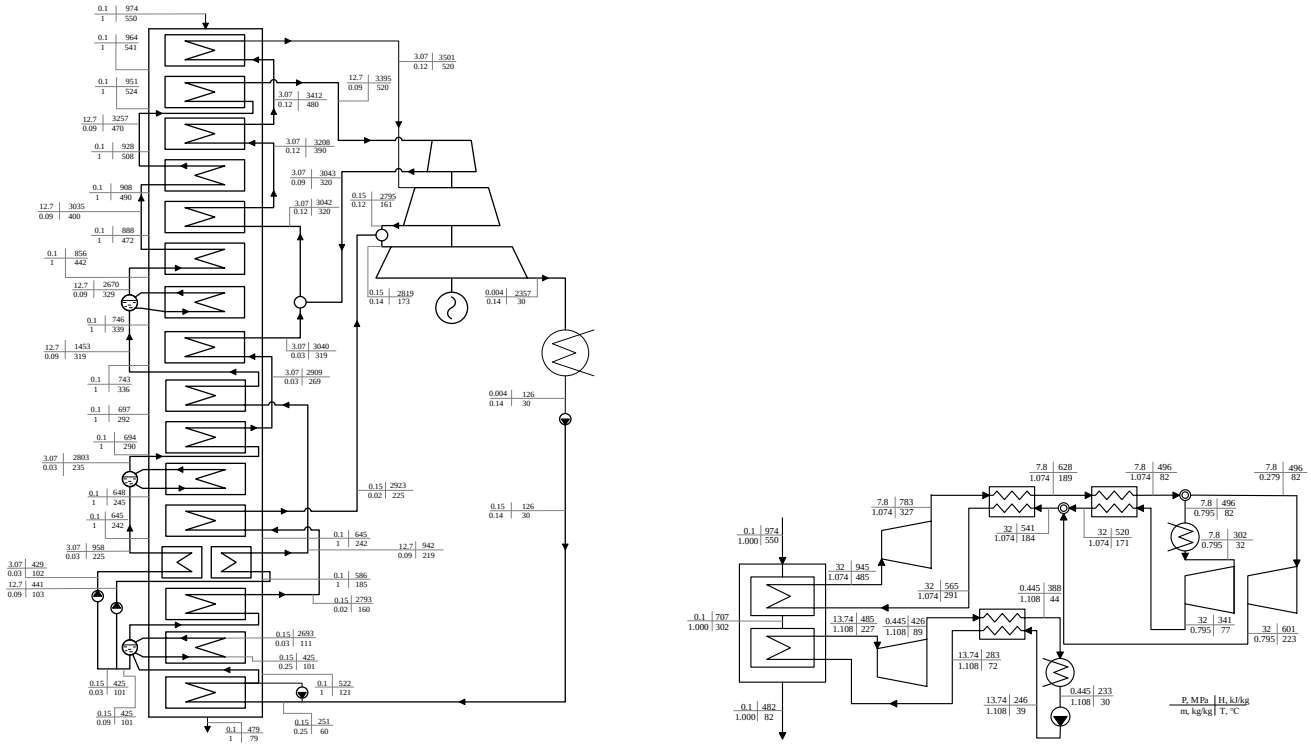


(**a**) $T_{ex} \geq 80$ °C (**b**) $T_{ex} \geq 150$ °C

Figure 22. Comparison of the specific power of power cycles at different temperatures of gases at the inlet and outlet of the waste heat boiler.

Thus, efficient utilization of waste heat for the production of electrical energy can be carried out, including in combined cycles, while the final choice of the structure and parameters of thermal circuits should be made on the basis of multiparameter optimization.

Figure 23 shows a comparison of the parameters in the key units of waste-to-energy plants operating on a steam-power cycle at three pressures and on a combined cycle from the Brayton recompression cycle on CO_2 and the ORC on R124 at a temperature of gases from the source $T_{g.in}$ = 550 °C and a temperature of exhaust gases not lower than T_{ex} > 80 °C. The net efficiency of the steam-power cycle with these parameters is 35% and of the combined cycle—33.3%.



(**a**) STU (**b**) SCO_2 + ORC

Figure 23. Parameters in the nodes of a three-pressure steam power cycle and a combined S–CO_2 + ORC cycle.

Under conditions where waste heat is transferred by air or a coolant, the deep cooling of which does not lead to the formation of condensate and acids (for example, gas turbine exhaust with high excess air), in the range of initial temperatures up to 300 °C the most efficient will be the use of organic Rankine cycles with a recuperator, and at higher temperatures up to $T_{g.in}$ = 520 °C—combined cycles consisting of the Brayton recompression cycle on S–CO_2 and the organic Rankine cycle with a recuperator, at higher initial temperatures the highest specific electric power during gas utilization is achieved using a steam power cycle with three pressure circuits (Figure 24). Under conditions where the gas cooling depth is limited by $T_{ex} \geq$ 150 °C, at gas temperatures up to 330 °C, the most efficient is the ORC with a recuperator, and at higher temperatures—the combined cycle.

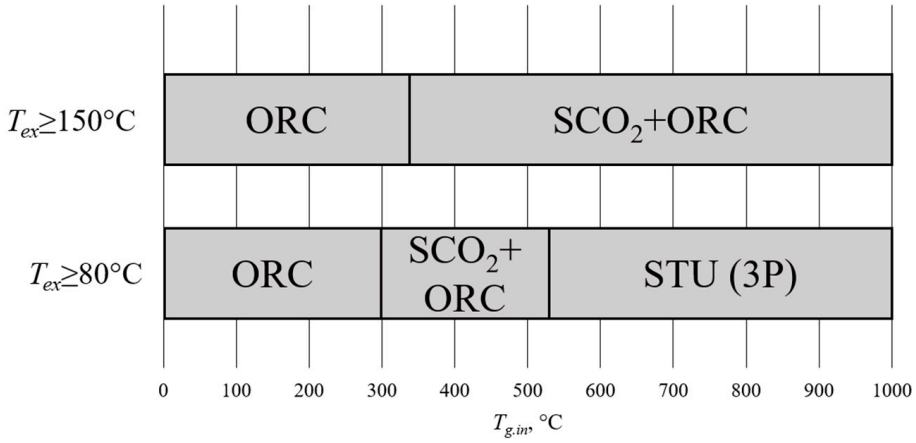
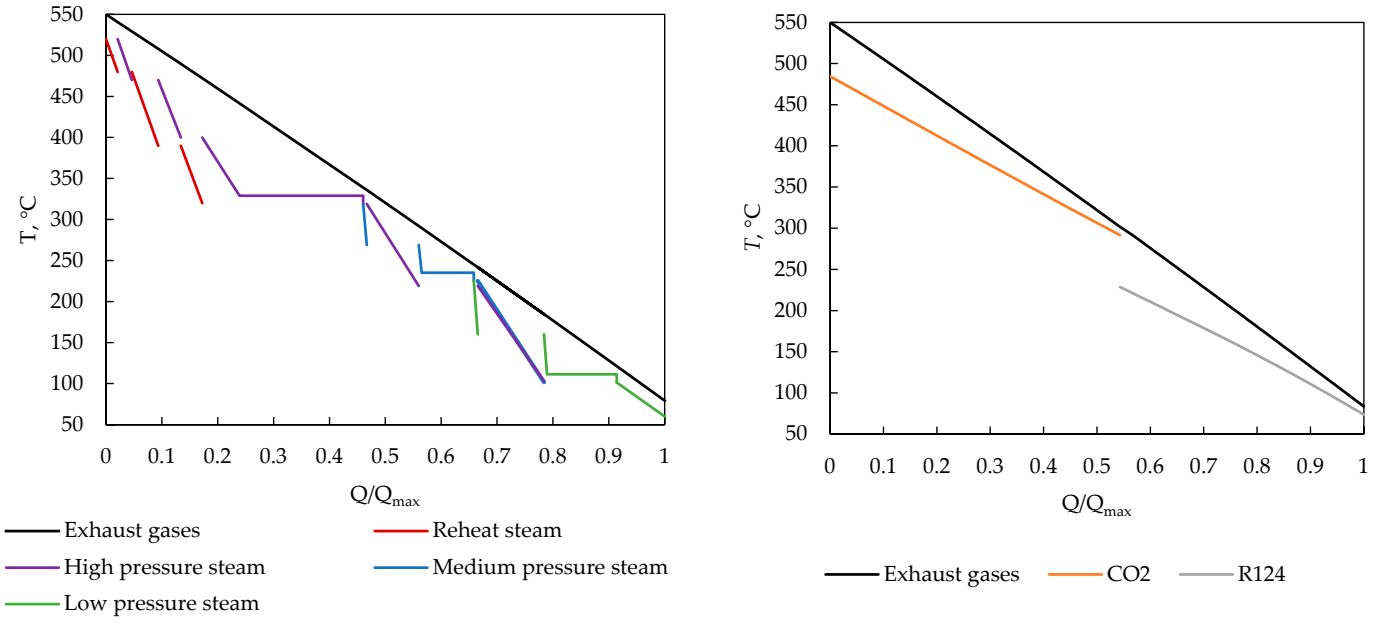


Figure 24. The most efficient power cycles at different temperatures of gases at the inlet and outlet of the waste heat boiler.

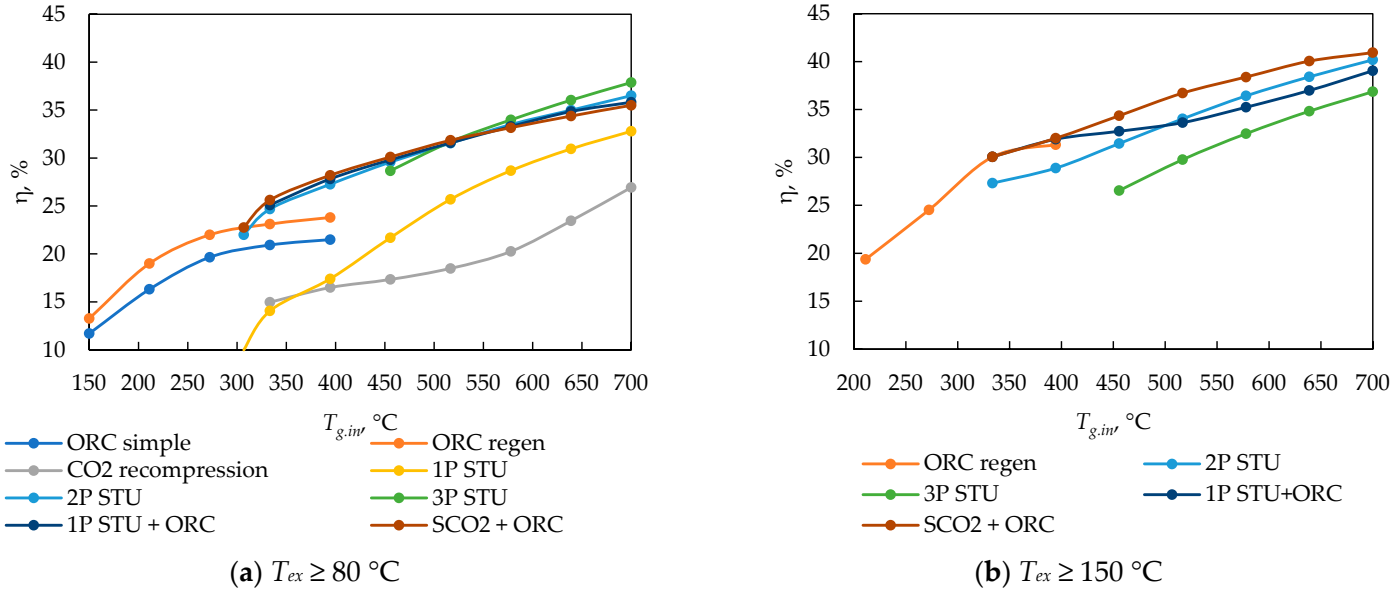
This is achieved primarily due to the fact that in the low-temperature region, the use of cycles on low-boiling coolants is more energy efficient: low critical parameters of organic media allow the implementation of a power cycle with a higher, compared to water vapor, heat supply temperature due to a smaller share of heat required for evaporation. At the same time, heat recovery in the ORC provides a higher level of efficiency compared to a simple cycle without a recuperator under conditions when the depth of gas cooling is limited. In the high-temperature part of the combined cycle, the use of the Brayton cycle on carbon dioxide is efficient due to several factors: high efficiency of recovery in HTR and LTR due to the use of recompression, as well as a high average integral temperature of heat supply to the cycle due to the absence of a phase transition in the supercritical cycle. Compared to the steam-power cycle, where there is practically no regenerative heating system, in the combined cycle, recuperation is achieved in both the high-temperature and low-temperature circuits. Figure 25 shows the T–Q diagram of the waste heat boilers for the circuits whose parameters are given in Figure 23. It is evident from the diagram that the average integral temperature of heat supply to the cycle in the second case is higher since the area limited by the gas cooling and heating lines of the working bodies of the power cycles is smaller. On the one hand, this determines energy efficiency, and on the other hand, it will require a significant increase in the heat exchange area in the waste heat boilers, which makes it necessary to economically substantiate the technical solutions under consideration.



(**a**) 3P STU (**b**) S–CO_2 + ORC

Figure 25. T–Q diagrams of waste heat boilers of a three-loop steam power cycle (**a**) and a combined cycle S–CO_2 + ORC (**b**).

The maximum level of energy efficiency of the considered power cycles for waste heat utilization varies in a wide range, depending on the initial and final temperatures of the gases. It is evident from Figure 26 that the ratio of the maximum specific electric power of the cycle to the maximum possible amount of thermal energy of the gases transferred to the cycle during cooling to 80 and 150 °C varies greatly depending on the choice of the working fluid and the scheme. When cooling to 80 °C, the net efficiency of the ORC with a recuperator changes from 13.4 to 23.8% with a change in $T_{g.in}$ from 150 to 400 °C, and when cooling to 150 °C, the efficiency changes from 19.4 at 210 °C to 31.3% at 400 °C. The efficiency of the combined cycle varies from 26 to 35% in the initial temperature range (350–700 °C) when cooling to 80 °C and from 31 to 41% when cooling to 150 °C.



(**a**) $T_{ex} \geq 80$ °C (**b**) $T_{ex} \geq 150$ °C

Figure 26. The net efficiency of waste heat recovery power cycles.

The results obtained allow us to make some recommendations on the choice of waste heat utilization technology for industrial enterprises. Table 3 presents the schemes and key parameters that can ensure the highest electrical output during waste heat utilization. In cases where gases contain sulfur compounds or when the water vapor content exceeds 5%, deep cooling in waste heat boilers is technically impossible. In such cases, the use of combined cycles with gas cooling to temperatures of at least 150 °C becomes effective. Thus, the combustion products of ferroalloy gas, gases of copper smelting furnaces, and pyrite roasting furnaces have a high content of sulfur compounds, and for such industrial enterprises, combined cycles should be used to utilize waste heat. At gas temperatures below 300–330 °C, the use of the organic Rankine cycle will be an effective solution. In conditions where the source temperature exceeds 700 °C, it is technically difficult to ensure a high temperature of the working fluid in the power cycle: today, the steam temperature at thermal power plants does not exceed 700 °C. For the correctness of the comparison, for high-temperature sources, the maximum temperature of the working fluid was limited to this value.

Table 3. Recommendations for the selection of the structure and parameters of the waste heat disposal plant in industrial enterprises.

Heat Source	Composition	Temperature, °C, (Enthalpy, kJ/m^3)	Power Cycle	Fluid	P_0, MPa	η, %
		Ferrous metallurgy				
Electric arc furnaces	CO = 5–70%; CO_2 = 5–15%; H_2 = 0.5–5%; O_2 = 3–10%	600–1800 (263–409)	STU 3P	steam	15/5/0.5	35–42
Ferroalloy gas combustion products	CO = 85%; H_2 = 4%; N_2 = 5.6%; O_2 = 1%; CO_2 = 3%; H_2S < 0.4%	1300–1600 (339–361)	S–CO_2 + ORC	CO_2, R124	32/10	40–45
Heating furnaces	CO_2 = 12.2%; H_2O = 17%; N_2 = 70%	800–1300 (305–368)	S–CO_2 + ORC	CO_2, R124	32/10	37–40

Table 3. *Cont.*

Heat Source	Composition	Temperature, °C, (Enthalpy, kJ/m^3)	Power Cycle	Fluid	P_0, MPa	η, %
Coke oven gas	CO_2 = 2–4%; CO = 6–8%; H_2 = 55–62%; N_2 = 2–3%; CH_4 = 24–28%	650–900 (336–410)	S–CO_2 + ORC	CO_2, R124	32/10	40–45
roasting furnaces	-	750–800	STU 3P	steam	15/5/0.5	37–42
Converter gas	CO = 58–90%; H_2O = 9%; N_2 = 10–13.6%; CO_2 = 15–18%	200–700 (151–319)	ORC/STU 3 P	R236ea/steam	15/5/0.5	20–38
Blast furnace gas	CO_2 = 10–13%; CO = 28–31%; H_2 = 4%; N_2 = 58–60%	150–350 (63–173)	ORC	R236ea	2–10	15–25
Blast furnace air heaters	-	200–300	ORC	R236ea/R124	3–10	17–25
Sintering machines	CO_2 = 4–10%; O_2 < 17%; CO < 3%; SO_x < 0.6%; NO_x < 0.2%; N_2 > 70%.	200–250 (98–127)	ORC	R236ea/R124	3–7	17–23
Non-ferrous metallurgy						
Pit furnaces of copper smelters	SO_2 = 10%; SO_3 < 2%; H_2O = 19%; CO_2 = 7%; N_2 = 62%	100–600 (337–355)	ORC/S–CO_2 + ORC	R236ea/CO_2, R124	32/10	15–42
Furnaces of copper smelters with a fluidized bed	-	800–900	S–CO_2 + ORC	CO_2, R124	32/10	40–45
Refining furnaces	CO = 10%; SO_2 = 5–12%; N_2 = 78%	1200–1400 (17–207)	S–CO_2 + ORC	CO_2, R124	32/10	40–45
Cement						
Cement clinker kilns	-	1000–1100 (362–375)	STU 3P	steam	15/5/0.5	37–42
Chemistry, petrochemistry, oil refining						
Pyrite roasting furnaces	SO_2 = 7–9%; O_2 = 9–11%; N_2 > 79%	650–900 (225–265)	S–CO_2 + ORC	CO_2, R124	32/10	40–45
Process gas generators	-	250–1100	STU 3P	R236ea (for $T_{g.in}$ < 330 °C), steam	3–10, 15/5/0.5	37–42
Tube furnaces for oil and fuel oil processing	CO = 2%; H_2 = 14%; N_2 = 82%	400–600 (179–234)	S–CO_2 + ORC, STU 3P	CO_2 + R124 (for $T_{g.in}$ < 550 °C), steam	28/8 15/5/0.5	37–42

The developed recommendations can ensure energy-efficient utilization of waste heat at industrial enterprises, but the final choice of technical solutions will be determined on the basis of assessments of the financial and economic indicators of the projects.

5. Conclusions

In this study, a thermodynamic analysis of power cycles for waste heat utilization was performed. Organic Rankine cycles, steam-water cycles, and cycles on supercritical carbon dioxide were considered. Prospects for the use of combined cycles were determined.

1. It was found that the use of organic Rankine cycles for waste heat utilization is an effective solution for the production of electric energy at an initial gas temperature of no more than 300 °C at a cooling temperature of up to 80 °C and no more than 330 °C when cooling to 150 °C. Based on the results of thermodynamic optimization, it was found that the highest electric power can be achieved using an organic Rankine cycle with a recuperator with freon R134a at an initial gas temperature of up to 150 °C, R236ea at a temperature of 150 to 200 °C, and R124 at higher temperatures.
2. Based on the results of the optimization of the Brayton recompression cycle on supercritical carbon dioxide, it was established that due to the high degree of heat recovery in the power cycle, the depth of gas cooling is limited. This leads to the fact that the final electric power of the cycle with recompression is lower than that of the cycle with one recuperator, in which the gases can be cooled to lower temperatures. Thus, the maximum thermal efficiency of the recompression cycle is achieved with a recompression fraction of 0.55–0.65 at an initial gas temperature of 300–500 °C, while the maximum electric power is in the complete absence of recompression. The value of the optimal pressure in this case is in the range of 30–35 MPa.
3. It was found that the combination of the Brayton recompression cycle on supercritical carbon dioxide with the organic Rankine cycle on R124 provides greater electric power than steam power cycles with three pressure circuits under conditions when the gas temperature is in the range of 300–550 °C at a cooling temperature of up to 80 °C, and when cooling gases with a high sulfur and moisture content to 150 °C, the combined cycle has greater electric power at a gas temperature of 330 °C and above. Higher efficiency of waste heat utilization in combined cycles is achieved when achieving optimal distribution of gas heat between the recompression and organic cycles. It was determined that the maximum sum of electric powers of the cycles under conditions when the recompression cycle accounts for 40–60% of the thermal energy of gases.
4. Based on thermodynamic optimization, recommendations were developed for choosing the structure and parameters of power cycles for utilizing waste heat of various industrial enterprises. At enterprises where the coolant has a high content of sulfur compounds or moisture and deep cooling of gases will lead to condensation—for example, at petrochemical and non-ferrous metallurgy enterprises—the use of combined cycles can ensure a utilization efficiency of up to 45%.

Author Contributions: Conceptualization, V.K. and N.R.; methodology, V.K.; software, A.V.; validation, V.K.; formal analysis, N.R.; investigation, I.M.; resources, A.R.; data curation, I.M.; writing—original draft preparation, I.M.; writing—review and editing, N.R.; visualization, A.V.; supervision, A.R.; project administration, A.R.; funding acquisition, A.R. All authors have read and agreed to the published version of the manuscript.

Funding: This study conducted by Moscow Power Engineering Institute was financially supported by the Ministry of Science and Higher Education of the Russian Federation (project No. FSWF-2023-0014, contract No. 075-03-2023-383, 18 January 2023).

Data Availability Statement: The original contributions presented in the study are included in the article material, further inquiries can be directed to the corresponding author.

Conflicts of Interest: The authors declare no conflicts of interest.

Nomenclature

Symbol	Description	Unit
$T_{g.in}$	inlet gas temperature	°C
T_{ex}	exhaust gases temperature	°C
P_0	initial pressure	MPa
η	cycle efficiency	%
m	specific mass flow rate	kg/kg
m^*	critical specific mass flow rate	kg/kg
N	specific net power	kJ/kg
Abbreviations		
ORC	Organic Rankine cycle	
HTR	High temperature recuperator	
LTR	Low temperature recuperator	
WHB	Waste heat boiler	
STU	Steam turbine unit	
HPC	High pressure cylinder	
LPC	Low pressure cylinder	
MPC	Medium pressure cylinder	

References

1. Eurostat. Available online: https://ec.europa.eu/eurostat/en/ (accessed on 7 October 2024).
2. Johnson, I.; Choate, W.T.; Davidson, A. *Waste Heat Recovery. Technology and Opportunities in US Industry*; BCS, Inc.: Laurel, MD, USA, 2008.
3. Liu, L.; Yuan, Y.; Kumar, S.; Wang, Z.; He, Y.; Lv, Y.; Liua, J.; Gul-e-Ranac, J.; Cen, K. Catalytic effect of metal chlorides on coal pyrolysis and gasification part II. Effects of acid washing on coal characteristics. *Thermochim. Acta* **2018**, *666*, 41–50. [CrossRef]
4. Li, J.; Ye, X.; Burra, K.G.; Lu, W.; Wang, Z.; Liu, X.; Gupta, A.K. Synergistic effects during co-pyrolysis and co-gasification of polypropylene and polystyrene. *Appl. Energy* **2023**, *336*, 120750. [CrossRef]
5. Panayiotou, G.P.; Bianchi, G.; Georgiou, G.; Aresti, L.; Argyrou, M.; Agathokleous, R.; Tsamos, K.M.; Tassou, S.A.; Florides, G.; Kalogirou, S.; et al. Preliminary Assessment of Waste Heat Potential in Major European Industries. *Energy Procedia* **2017**, *123*, 335–345. [CrossRef]
6. Su, Z.; Zhang, M.; Xu, P.; Zhao, Z.; Wang, Z.; Huang, H.; Ouyang, T. Opportunities and Strategies for Multigrade Waste Heat Utilization in Various Industries: A Recent Review. *Energy Convers. Manag.* **2021**, *229*, 113769. [CrossRef]
7. Wieland, C.; Schifflechner, C.; Dawo, F.; Astolfi, M. The Organic Rankine Cycle Power Systems Market: Recent Developments and Future Perspectives. *Appl. Therm. Eng.* **2023**, *224*, 119980. [CrossRef]
8. Exergy's ORC Systems Case Studies. Exergy. Available online: https://www.exergy-orc.com/reference/case-studies/ (accessed on 7 October 2024).
9. TURBODEN Combined Cycle Power Plant | Combined Power Cycle. Available online: https://www.turboden.com/solutions/2603/combined-cycles (accessed on 28 July 2024).
10. Heat ReCycle Solutions. Available online: https://www.siemens-energy.com/global/en/home/products-services/product/heat-recycle-solutions.html (accessed on 28 July 2024).
11. Kindra, V.; Rogalev, N.; Rogalev, A.; Naumov, V.; Sabanova, E. Thermodynamic Optimization of Low-Temperature Cycles for the Power Industry. *Energies* **2022**, *15*, 2979. [CrossRef]
12. Wei, D.; Lu, X.; Lu, Z.; Gu, J. Performance Analysis and Optimization of Organic Rankine Cycle (ORC) for Waste Heat Recovery. *Energy Convers. Manag.* **2007**, *48*, 1113–1119. [CrossRef]
13. Karellas, S.; Leontaritis, A.-D.; Panousis, G.; Bellos, E.; Kakaras, E. Energetic and Exergetic Analysis of Waste Heat Recovery Systems in the Cement Industry. *Energy* **2013**, *58*, 147–156. [CrossRef]
14. Wang, E.H.; Zhang, H.G.; Fan, B.Y.; Ouyang, M.G.; Zhao, Y.; Mu, Q.H. Study of working fluid selection of organic Rankine cycle (ORC) for engine waste heat recovery. *Energy* **2011**, *36*, 3406–3418. [CrossRef]
15. Angelino, G. Carbon Dioxide Condensation Cycles For Power Production. *J. Eng. Power* **1968**, *90*, 287–295. [CrossRef]
16. Angelino, G. Real Gas Effects in Carbon Dioxide Cycles. In Proceedings of the ASME 1969 Gas Turbine Conference and Products Show, Cleveland, OH, USA, 9–13 March 1969; American Society of Mechanical Engineers. p. V001T01A071.
17. Kulhanek, M.; Dostal, V. Supercritical Carbon Dioxide Cycles Thermodynamic Analysis and Comparison. In Proceedings of the Supercritical CO_2 Power Cycle Symposium, Boulder, CO, USA, 24–25 May 2011; pp. 24–25.
18. Rogalev, N.; Rogalev, A.; Kindra, V.; Komarov, I.; Zlyvko, O. Structural and Parametric Optimization of S–CO_2 Nuclear Power Plants. *Entropy* **2021**, *23*, 1079. [CrossRef] [PubMed]
19. Song, J.; Li, X.; Ren, X.; Gu, C. Performance Improvement of a Preheating Supercritical CO_2 (S–CO_2) Cycle Based System for Engine Waste Heat Recovery. *Energy Convers. Manag.* **2018**, *161*, 225–233. [CrossRef]

20. Kindra, V.; Maksimov, I.; Komarov, I.; Xu, C.; Xin, T. Feasibility Study of Scheme and Regenerator Parameters for Trinary Power Cycles. *Energies* **2023**, *16*, 3886. [CrossRef]
21. Cho, S.K.; Kim, M.; Baik, S.; Ahn, Y.; Lee, J.I. Investigation of the Bottoming Cycle for High Efficiency Combined Cycle Gas Turbine System with Supercritical Carbon Dioxide Power Cycle. In Proceedings of the Turbo Expo: Power for Land, Sea, and Air, Montreal, QC, Canada, 15–19 June 2015; American Society of Mechanical Engineers. Volume 56802, p. V009T36A011.

Disclaimer/Publisher's Note: The statements, opinions and data contained in all publications are solely those of the individual author(s) and contributor(s) and not of MDPI and/or the editor(s). MDPI and/or the editor(s) disclaim responsibility for any injury to people or property resulting from any ideas, methods, instructions or products referred to in the content.